The Pennsylvania State University

The Graduate School

Department of Chemistry

COPOLYMERIZATION OF POLAR AND NON-POLAR MONOMERS: FREE RADICAL POLYMERIZATION AND LATE TRANSITION CATALYZED INSERTION POLYMERIZATION

A Dissertation in

Chemistry

by

Rong Luo

Submitted in Partial Fulfillment
of the Requirements
for the Degree of

Doctor of Philosophy

December 2008

The dissertation of Rong Luo was reviewed and approved* by the following:

Ayusman Sen
Professor of Chemistry
Head of the Department of Chemistry
Thesis Advisor
Chair of Committee

Harry Allcock
Professor of Chemistry

John Badding
Associate Professor of Chemistry

T. C. Mike Chung
Professor of Material Science and Engineering

*Signatures are on file in the Graduate School

ABSTRACT

The addition of the heterogeneous Lewis acid, acidic alumina (Acidic, Brockmann I, standard grade, ~ 150 mesh, pH = 4.5±0.5 in aqueous solution) to the 2, 2'-azobis (2-methylpropionitrile) (AIBN) -initiated copolymerization of methyl acrylate (MA) with 1-alkenes results in significant increase in polymerization rate and increased incorporation of the later monomer to the polymer backbone. Alumina can be recovered by filtration and reused repeatedly with no loss of activity. This led to the design of an Al_2O_3-filled column reactor system for the copolymerization reaction

The addition of insoluble acidic alumina to controlled radical NMP and RAFT polymerizations of acrylate monomers results in significantly higher reaction rates and conversions. The effect is particularly dramatic since only a small fraction of the Lewis acid sites that are present on the alumina surface can actually interact with the acrylate. The Lewis acid-enhanced polymerizations have "living" characteristics, allowing the synthesis of block copolymers. The alumina can be quantitatively removed by filtration and recycled with no significant loss in efficacy.

The addition of both homogeneous and heterogeneous Brønsted acids resulted in increased monomer conversion and 1-alkene incorporation. Further, the heterogeneous Brønsted acids can be recycled without loss of activity. A direct correlation exists between the ability of the Lewis or Brønsted acid to bind to the ester group of the acrylate/methacrylate monomer and its ability to promote the copolymerization reaction. For Lewis acids, there is also a direct

correlation between the charge/size ratio at the metal center and their ability to promote copolymerizations.

The first electron transfer induced iron-catalyzed atom transfer radical polymerization (ATRP) system for styrene derivatives was developed. Environmental benign reducing agents tin(II) 2-ethylhexanoate ($Sn(EH)_2$) and D-glucose were employed to constantly regenerate active Fe(II) species. This reducing/reactivating cycle allowed the controlled polymerization even in the presence of a limited amount of air. Furthermore, the amount of iron catalyst could be reduced to as low as 0.01 mmol while retaining sufficient control over the polymerization. Monomers with electron-withdrawing substituents polymerized faster than those having electron-donating substituents. Block copolymers were obtained by chain extension of polystyrene macroinitiators. Well-defined copolymers of styrene and methyl methacrylate (MMA) were also synthesized using this iron-based catalyst, and the MMA content in the copolymers could be varied by changing the monomer feed ratio.

The palladium-catalyzed alternating copolymerization of ethene and carbon monoxide has been extensively studied in the last two decades. A series of polyketones with very low CO content has been synthesized using palladium catalyst bearing ($P\text{-}SO_3^-$) ligand by varying the monomer feed ratio and reaction conditions. We have also demonstrated that the reason for the non-alternation in this system is more complicated than just the instability of the five-membered chelate resting state existed in the catalytic cycle, and the less dramatic difference in CO and ethene binding affinity also plays an important role for this non-alternating fashion. The kinetics and thermodynamic data has allowed us to estimate the fraction of non-alternation due to double ethene insertion during the copolymerization.

TABLE OF CONTENTS

LIST OF FIGURES

LIST OF TABLES

ACKNOWLEDGEMENTS

The thesis dissertation marks the end of a long and eventful journey for which there are many people that I would like to acknowledge for their support along the way. Foremost, I would like to thank my advisor, Dr. Ayusman Sen, who has been a significant presence in my life. I will always be thankful for his encouragements, support, and lots of good ideas throughout my Ph.D study. I have also enjoyed working with all the former and current Sen group members. I would specifically like to thank my "polymer subgroup" colleagues, Dr. Megan Nagel, Dr. Sachin Borkar, David Newsham and Ying Chen for their help, advice and effort.

I wish to thank the Rohm & Hass Company and LG Chem for their active collaboration and money support. People from these two companies helped me to realize the importance of my own research. The accomplishments I acquired through such collaborations have offered me a lot of confidence for my future career pursuit. I would also like to acknowledge the National Science Foundation, the Department of Energy and the Dalalian Research fellowship for their generous funding support for my graduate study.

Lastly, and most importantly, I want to thank my family. To my Mom and Dad, Zhiyu Li and Shenghua Luo, your tremendous support and unconditional love is and will always be inspiring me. It is so natural to follow the path to a Ph.D in such an excellent environment you created for me, but I feel so guilty for the long absence at home in the last four years. For this and much more, I am forever in your debt. To my husband, Rui Zhang, your endless love and encouragement has made all these meaningful to me. You don't know how grateful I am and how fortunate I feel when you gave up everything you had in China and came to the US just for me. I would like to thank you for your incredible patience with me, solving all my computer problems,

helping with the formatting of my papers and thesis, commuting eight hours on the road just to spend the weekend with me. To my family, I dedicate this thesis.

Chapter 1

Introduction

Despite the size and the commodity nature, poly(1-alkenes) (also known as polyolefins) are still the fastest-growing segment of polymer industry. A paramount target in polyolefin research is the controlled copolymerization of simple olefins with polar functional monomers, because polar functional groups control a variety of important polymer properties, such as toughness, adhesion, barrier properties, surface properties, solvent resistance, miscibility with other materials, and rheological properties.[1-3]

However, the copolymerization of polar monomers and non-polar 1-alkenes is by no means a trivial task. The inherent difficulty arises from the very different polymerization mechanisms though which these two classes of monomers normally undergo polymerization. Polar monomers such as acrylates and methacrylates are readily polymerized by free radical polymerization, while simple 1-alkenes such as ethene and propylene undergo radical polymerization only under very harsh reaction conditions to yield branched products. On the other hand, simple 1-alkenes are polymerized by early transition metal catalyst through insertion mechanism. The early transition metal catalysts are highly oxophilic in nature and have very limited polar functionality tolerance.

In order to achieve the successful copolymerization of polar and non-polar monomers, efforts have been made to develop late transition metal catalysts which are less oxophilic in nature and more functionality tolerant. In 1998, Brookhart reported a cationic palladium (II) α-diimine complex which could copolymerize methyl acrylate and ethene to yield highly branched products.[4] Later in 2002, Drent reported a neutral palladium phosphine sulfonate complex which could make linear copolymer of methyl acrylate and ethene.[5] In both cases, the methyl acrylate

incorporation is less than 17%. A much powerful method to achieve the copolymerization of polar monomers and non-polar 1-alkenes is the free radical polymerization which involves the use of a strong Lewis acid as a complexation agent. Recently, our group has shown that the presence of a catalytic amount of the Lewis acid, $Sc(OTf)_3$, leads to increased reaction rate and increased incorporation of the non-polar 1-alkene.[6]

The general theme of this thesis deals with the controlled radical copolymerization of polar and non-polar monomers in the presence heterogeneous, recyclable Lewis acid and the mechanistic study of the late transition metal catalyzed insertion copolymerization of carbon monoxide and ethene. Chapter 2 describes the copolymerization of acrylate and simple 1-alkenes in the presence of heterogeneous and recyclable acidic alumina. Continuing the work of Chapter 2, Chapter 3 achieves the rate enhancement of controlled radical polymerization of acrylate in the presence of the recyclable acidic alumina. Chapter 4 summarizes the effects of Lewis and Brønsted acids on the homopolymerization of acrylates and their copolymerization with 1-alkenes. On a different note, Chapter 5 covers the design of an electron transfer induced iron-based atom transfer radical polymerization catalyst for styrene derivatives. Finally, Chapter 6 details the mechanistic study for the palladium catalyzed non-alternating copolymeriztion of carbon monoxide and ethene.

Although it has been shown that the presence of a Lewis acid serves to increase the copolymer yield and the incorporation of the non-polar alkene, most Lewis acids employed thus far are relatively expensive materials that are soluble in the reaction medium and, therefore, not easily recycled. Chapter 2 describes the use of a heterogeneous Lewis acid, acidic alumina, for these copolymerization reactions. The bonding of the acrylate monomer to the surface of Lewis acid site greatly improved its reactivity, therefore, under ideal conditions, the acrylate monomer that participate in the polymerization would be predominantly those that are bound to the heterogeneous Lewis acid. The addition of the acidic alumina to the 2, 2'-azobis(2-

methylpropionitrile) (AIBN) -initiated copolymerization of methyl acrylate with 1-alkenes results in significant increase in polymerization rate and increased incorporation of the non-polar monomer into the polymer backbone. The acidic alumina can be recycled repeatedly without loss of activity. Based on this observation, we also explored the possibility of using an acidic Al_2O_3 filled column as a reactor system.

In Chapter 3, acidic alumina was employed for the rate enhancement of controlled radical polymerizations of acrylates Significant rate enhancementss for both nitroxide-mediated polymerization (NMP) and reversible addition-fragmentation chain transfer (RAFT) polymerization were achieved in the presence of a catalytic amount of acidic alumina. The Lewis acid-enhanced polymerizations have "living" characteristics, allowing the synthesis of block copolymers. The alumina can be quantitatively removed by filtration and recycled with no significant loss in efficacy.

In Chapter 4, we report the first copolymerization of acrylate and methacrylate with non-polar 1-alkenes in the presence of recyclable heterogeneous Brønsted acids as complexation agents. The use of either homogeneous Brønsted acids, such as pyridinium triflate (PyH), or heterogeneous Brønsted acids, such as crosslinked poly(4-vinylpyridinium p-toluenesulfonate) (PPyH) or Nafion, resulted in the copolymerizations proceeding with higher conversion and increased 1-alkene incorporation. Further, the heterogeneous Brønsted acids can be recycled repeatedly without attenuation of activity. We also examined the relationship between the complexing ability of the Lewis and Brønsted acids vis-à-vis the carbonyl group of the ester functionality and their ability to promote acrylate and methacrylate homo- and copolymerizations and we found a direct correlation between the two. Likewise, for soluble Lewis acids, there is a direct correlation between the charge/size ratios at the metal center their ability to promote

copolymerizations. Thus, this study provides a semi-quantitative way of estimating the efficacy of a given Lewis or Brønsted acid in promoting acrylate/methacrylate polymerizations.

Chapter 5 described an electron transfer induced iron-catalyzed atom transfer radical polymerization (ATRP) system for styrene derivatives. From the stand point of "Green Chemistry", the environmentally benign reducing agents tin(II) 2-ethylhexanoate ($Sn(EH)_2$) and D-glucose were employed to constantly regenerate active Fe(II) species. The addition of a reducing agent keeps a constant concentration of the activating species, allowing the polymerization to be sufficiently controlled even in the presence of a limited amount of air or with very low concentration of iron catalyst. The substituent effect on polymerization rate was studied via the Hammett plot. Block copolymers were obtained by chain extension of polystyrene macroinitiators. Well-defined copolymers of styrene and methyl methacrylate (MMA) were also synthesized using this iron-based catalyst, and the MMA content in the copolymers could be varied by changing the monomer feed ratio.

The final Chapter describes a mechanistic study of non-alternating copolymerization of ethene and carbon monoxide (CO). Radom copolymerization of CO and ethene with very low CO content has long been a goal of polyketone research, since such copolymer possesses desirable yet unattainable properties and allows further functionalizations.[7] A series of polyketones with very low CO content has been synthesized using a palladium catalyst bearing a phosphine sulfonate ($P{\sim}SO_3^-$) ligand by varying the monomer feed ratio and reaction conditions. We have also demonstrated that the reason for the non-alternation in this system is more complicated than just the instability of the five-membered chelate resting state, and the unusual small difference in ethene and CO binding affinity also plays an important role in determining the final polymer composition. The kinetic and thermodynamic data has allowed us to estimate the fraction of non-alternation due to double ethene insertion during the copolymerization.

1.1 References

1. Boffa, L. S.; Novak, B. M. *Chem. Rev.* **2000**, *100*, 1479-1493.

2. Ittel, S. D; Johnson, L. K.; Brookhart, M. *Chem. Rev.* **2000**, *100*, 1169-1204.

3. Liu, S.; Sen, A . *J. Polym. Sci., Part A: Polym. Chem.* **2004**, *42*, 6175-6192.

4. Mecking, S.; Johnson, L.K.; Wang, L.; Brookhart, M. *J. Am. Chem. Soc.* **1998**, *120*, 888-899.

5. Drent, E.; Dijik, R.V.; Ginkel, R.V.; Oort, B.V.; Pugh, R.I. *Chem. Commun.* **2002**, 744-745.

6. Nagel, M.; Poli, D.; Sen, A. *Macromolecules* **2005**, 38, 3029-3032.

7. (a) Catalytic Synthesis of Alkene-Carbon Monoxide Copolymers and Cooligomers; Sen, A., Ed.; Catalysis by Metal Complexes 27; Kluwer Academic: Dordrecht, 2003. (b) Mul, W. P.; Oosterbeck, H.; Betel, G. A.; Kramer, G.-J.; Drent, E. *Angew. Chem., Int. Ed.* **2000**, *39*, 1848–1851.

Chapter 2

Recyclable, Heterogeneous Lewis Acid-Mediated Copolymerization of Acrylates and Non-polar Alkenes

2.1 Introduction

The physical and chemical properties of polymers are significantly influenced by their microstructures. In this context, the synthesis of copolymers of acrylates with simple alkenes with predictable compositions and structures is of great current interest because the combination of the two classes of monomers can greatly enhance the range of currently attainable polymer properties[1-3]. We[4-9] and others[10-12] have reported the free radical copolymerization of acrylates with ethene and 1-alkenes. Random acrylate-rich copolymers in relatively low yield were obtained. More recently, we have shown that the presence of a catalytic amount of the Lewis acid, $Sc(OTf)_3$, leads to increased reaction rate and increased incorporation of the non-polar alkene[9]. Thus, essentially alternating copolymers in good yield can be obtained. The Lewis acid coordinates to the ester carbonyl group of the acrylate monomer and reduces the electron density in the conjugated C=C bond, thereby (a) increasing the reactivity of the radical generated there from and (b) making the radical more susceptible to attack by the relatively electron-rich non-polar alkene.[13]

Although the presence of a Lewis acid serves to increase the copolymer yield and the incorporation of the non-polar alkene, most Lewis acids[9, 13-18] employed thus far are relatively expensive materials that are soluble in the reaction medium and, therefore, not easily recycled. From the standpoint of practical "Green Chemistry," the ideal Lewis acid should be insoluble that

can be separated by filtration and reused.[19] At first glance, this appears to be a difficult problem because the radical polymerization would be expected to occur in the liquid monomer phase and the insoluble Lewis acid would be expected to have a minimal influence on the polymerization. However, as discussed above, the bonding of the acrylate monomer to the Lewis acid significantly increases its reactivity. Thus, under ideal conditions, the acrylate monomer units that participate in the polymerization would be predominantly those that are bound to the heterogeneous Lewis acid.

We investigated the copolymerization of methyl acrylate (MA) and with non-polar ethene and 1-alkenes in the presence of solid acidic alumina (Al_2O_3) as Lewis acid. The copolymerization proceeds with increased 1-alkene incorporation and increased acrylate conversion. Most importantly, acidic alumina can be recycled repeatedly with no loss of activity. This led to the design of an Al_2O_3-filled column reactor system for the copolymerization reactions.

2.2 Results and Discussion

2.2.1 Homopolymerization of Methyl Acrylate

The addition of acidic alumina (Aldrich, acidic, Brockmann I, standard grade, ~ 150 mesh, pH = 4.5±0.5 in aqueous solution) to the AIBN-initiated homopolymerization of methyl acrylate led to a significant increase in polymerization rate and conversion; however, the tacticity of the resultant polymer was unaffected (Table **2-1**). Clearly, even a Lewis acid that is insoluble in the reaction medium can still increase the reactivity of the propagating radical by coordination through the ester carbonyl group. The effect is particularly dramatic since only a small fraction of the Lewis acid sites that are present on the alumina surface can actually interact with the acrylate.

Table **2-1**: Homopolymerization of methyl acrylate (MA) in the presence and absence of acidic Al_2O_3[a]

Entry	$\frac{[Al_2O_3]}{[MA]}$	Yield (%)	M_n[b] (x 10^{-4})	M_w/M_n[b]	Tacticity[c]		
					mm	mr	rr
1	0	42	1.7	2.23	29	44	27
2	1: 5	58	1.6	2.37	28	42	30
3	1: 2	83	1.9	2.22	30	42	28

aConditions: MA, 0.3 g; AIBN, 0.005 g; PhCl, 5 ml; 75 ^{o}C , 18h. bBy GPC using polystyrene

Although it has been assumed that the monomers should have more mobility than the propagating radical chains, our observation would appear to contradict such scenario. One possible explanation would be that the propagating radical chain end preferentially reacts with the coordinated monomers on the surface of the heterogeneous Lewis acid.

2.2.2 Copolymerization of Methyl Acrylate with 1-Alkenes

The effect of added acidic alumina to the AIBN-initiated copolymerization of methyl acrylate (MA) with ethene at three different temperatures was examined (Table **2-2**). The copolymer compositions were determined from ^{1}H-NMR integration of the methoxy protons versus aliphatic resonances. Irrespective of the reaction temperature, the ethene incorporation and, especially, the copolymer yield increased significantly upon the addition of alumina. The copolymer microstructure was examined by ^{1}H and ^{13}C-NMR spectroscopy. At high ethene incorporation, the structure was nearly alternating. The ^{13}C NMR spectrum showed five major resonance at 175.9 (-C(O)-), 51.8 (-OCH_3), 45.6 (-CH-), 32.5 (-CH_2-), 25.5 (-CH_2-) ppm from alternating MA-ethene copolymer sequence. Less intense peaks were observed at 43.6 and 35.0 ppm attributable to consecutive MA units and even lower intensity peaks at 29.8 and 27.7 ppm attributable to consecutive ethene units, suggesting a small degree of non-alternation. A similar microstructure was previously observed for $Sc(OTf)_3$-mediated radical copolymerization of MA with ethene.[9] Table 2.3 summarizes the results for the copolymerization of ethene, 1-hexene, and 1-decene with MA in the presence and absence of acidic alumina at 75 ^{o}C. Again, a dramatic increase (approx. 2-3 x higher) in monomer conversion was observed in the presence of the Lewis acid, irrespective of the alkene employed. Furthermore, the alumina could be recovered by simple filtration and reused with no attenuation of activity (entries 4 and 11, Table **2-3**). Note that while

the polymerizations were routinely allowed to proceed for 18 h, entries 5, 7 and 9 in Table **2-3** suggest that the reactions are completed in the first 4 h.

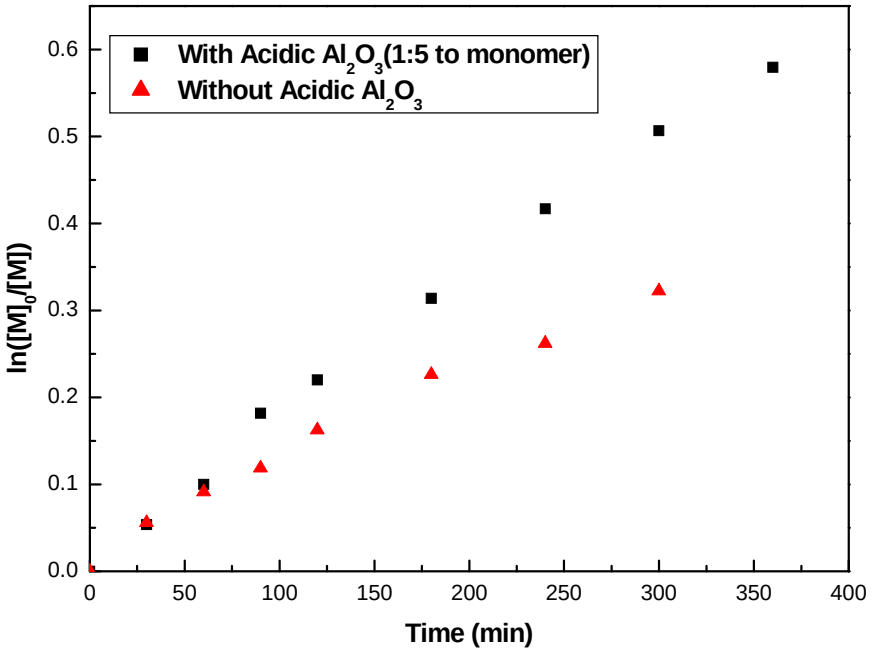

Figure **2-1**: Effect of added alumina on the rate of AIBN-initiated copolymerization of methyl acrylate with 1-hexene. Conditions: MA, 0.9 g; 1-hexene, 3.0 g; AIBN, 0.015 g; PhCl, 20 ml; 60 ^{o}C .

Table **2-2**: Copolymerization of methyl acrylate (MA) with ethene in the presence and absence of acidic Al_2O_3 at different temperatures[a]

Entry	Temp. (^oC)	$\frac{[Al_2O_3]}{[MA]}$	Yield (g)	Ethene incorp. (mol%)	MA conv. (%)	M_n[b] (x 10^{-4})	M_w/M_n[b]
1	60	0	0.084	35	23	12.6	1.57
2	60	1:5	0.189	35	54	10.7	1.49
3	60	1:2	0.223	43	60	4.6	1.87
4	75	0	0.140	40	39	9.4	1.57
5	75	1:5	0.212	45	56	3.5	1.86
6	75	1:2	0.232	45	61	3.4	1.75
7	90	0	0.186	44	50	5.4	1.60
8	90	1:5	0.292	46	76	2.5	1.85
9	90	1:2	0.304	48	78	2.3	1.71

[a]Conditions: MA, 0.3 g; Ethene, 500 psi; AIBN, 0.005 g; PhCl, 5 ml; 18 h. [b]By GPC using polystyrene standards.

Table**2-3**: Copolymerization of methyl acrylate (MA) with 1-alkenes in the presence and absence of acidic Al_2O_3[a]

Entry	Alkene (psi or g)	$\frac{[Al_2O_3]}{[MA]}$	Yield (g)	Alkene incorp. (mol%)	MA conv. (%)	M_n[d] (x 10^{-4})	M_w/M_n[d]	Al_2O_3 recovered (%)
1	Ethene (500)	0	0.140	40	39	9.4	1.57	-
2	Ethene (500)	1:5	0.212	45	56	3.5	1.86	93.8
3	Ethene (500)	1:2	0.232	45	61	3.4	1.75	90.6
4[b]	**Ethene (500)**	**1:2**	**0.223**	**47**	**58**	**9.6**	**1.43**	**95.1**
5[c]	1-Hexene (1.0)	0	0.061	31	14	2.0	1.75	-
6	1-Hexene (1.0)	0	0.050	29	11	3.0	1.78	-
7[c]	1-Hexene (1.0)	1:5	0.146	31	34	2.8	1.54	89.0
8	1-Hexene (1.0)	1:5	0.138	32	32	1.3	2.24	83.2
9[c]	1-Hexene (1.0)	1:2	0.179	33	40	2.5	1.71	98.1
10	1-Hexene (1.0)	1:2	0.176	35	38	1.6	2.37	90.2
11[b]	**1-Hexene (1.0)**	**1:2**	**0.152**	**35**	**33**	**1.1**	**1.97**	**94.4**
12	1-Decene (1.5)	0	0.071	27	15	1.2	2.24	-
13	1-Decene (1.5)	1:5	0.131	32	25	1.0	2.19	94.4
14	1-Decene (1.5)	1:2	0.176	32	33	1.2	2.34	89.8

[a]Conditions: MA, 0.3 g; AIBN, 0.005 g; PhCl, 5 ml; 75 °C , 18 h. [b]Using recycled Al_2O_3. [c]Run for 4 h. [d]By GPC using polystyrene standards.

2.2.3 Design of Column Reactor

Our observation that relatively inexpensive, air-stable, alumina can be used to significantly increase the yield of MA/alkene copolymers prompted us to explore the possibility of employing an alumina-filled column as a reactor system (Figure **2-2**). The concept was to carry out the copolymerization inside the column, wash out the copolymer formed subsequently, and reuse the column for another copolymerization. Results of these experiments are summarized in Table **2-4**. While there are some variations in polymer yields, especially in the beginning, after several cycles copolymer with 30 mol% incorporation of 1-hexene was obtained with an approximately steady 25-30% acrylate conversion. The conversion was lower than that observed in batch reactors; nevertheless it was 2 x higher than that observed in the absence of alumina (entry 5 and 6, Table **2-3**).

The variation in yield observed in Table **2-4** may be ascribed to incomplete removal of the polymer formed on the alumina surface. However, if the alumina surface was indeed covered with polymer, its ability to activate the acrylate monomer through coordination to the ester group would be quenched. The clear trend of increased polymer yield in the column reactor through many cycles when compared to the yield in the absence of alumina would appear to rule out such a scenario.

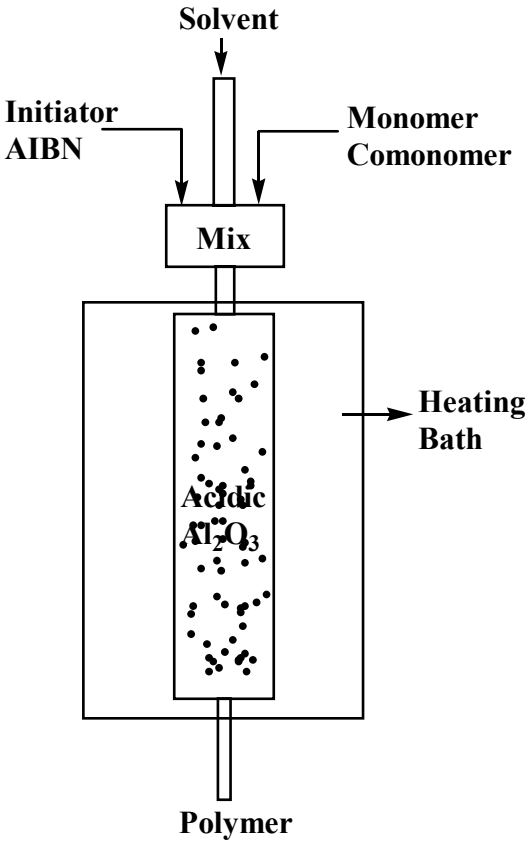

Figure**2-2**: Alumina-filled column reactor

Table**2-4**: **C**opolymerization of methyl acrylate (MA) with 1-hexene in an alumina-filled column[a]

Recycling round	MA (g)	1-Hexene (g)	Yield (g)	Hexene Incorp. (mol %)	MA Conv. (%)	M_n[b] (x 10^{-4})	M_w/M_n[b]
2	1.00	3.00	0.152	33	10	6.5	1.77
3	1.00	3.00	0.300	32	21	4.8	2.52
4	1.00	3.00	0.255	33	17	1.9	2.84
5	1.00	3.00	0.443	33	30	1.7	3.11
6	1.00	3.00	0.253	29	18	2.7	2.49
7	1.00	3.00	0.277	29	20	3.9	2.17
8	1.00	3.00	0.328	29	24	3.1	2.40
9	1.00	3.00	0.328	27	24	3.1	2.13
10	1.00	3.00	0.475	31	33	1.6	2.81
11	1.00	3.00	0.403	30	29	1.7	2.81
12	1.00	3.00	0.395	30	28	2.4	2.63

[a]Conditions: AIBN, 0.005 g; PhCl, 5 ml; 60 °C , 18 h. [b]By GPC using polystyrene standards.

2.3 Conclusion

In summary, the addition of the insoluble Lewis acid, acidic alumina, to the AIBN-initiated homo- and copolymerizations of acrylate with non-polar 1-alkenes, resulted in increased monomer conversion and increased incorporation of the latter monomer into the polymer backbone. Alumina can be recovered by filtration and reused repeatedly with no loss of activity. This led to the design of an Al_2O_3-filled column reactor system for the copolymerization reactions. In principal, the latter can be modified into a flow-reactor where the polymerization occurs in the column and the polymer solution flows out and is continuously replaced by fresh solution containing the monomers and initiator.

2.4 Experimental Procedure

2.4.1 Materials

All chemicals and reagents were obtained from Aldrich unless otherwise stated. Methyl acrylate (MA, 99%), 1-hexene, and 1-decene were vacuum distilled from CaH_2 and stored under N_2. 2, 2'-Azobis(isobutyronitrile) (AIBN, 98%), and aluminum oxide (activated, acidic, Brockmann I, standard grade, ~ 150 mesh, pH = 4.5±0.5 in aqueous solution) was used as received.

2.4.2 Instrumentation

^{1}H- and ^{13}C-NMR spectra were recorded using a Bruker 300-DPX spectrometer at ambient temperature (^{1}H-NMR, 300MHz; ^{13}C-NMR, 75 MHz). Chemical shifts are referenced to $CDCl_3$. Molecular weights and molecular weight distributions were determined on a Shimadzu gel permeation chromatography (GPC) chromatograph containing a three-column bed (styragel HR 7.8 × 300 mm columns with 5 μm beads size; 100-5000, 500-30,000, and 2,000-4 × 10^6 Da), a Shimadzu RDI-10A differential refractometer, and a Shimadzu SPD-10A tunable absorbance detector (254 nm). GPC samples were run in tetrahydrofuran at a flow rate of 1 ml/min at 35 ^{o}C and calibrated against polystyrene standards. Analysis was done using EZSTART 7.2 software. Gas chromatography(GC) analysis was performed on an Agilent 5890 Series II GC. The samples were heated from 40 ^{o}C to 100 ^{o}C at a ramp rate of 4 ^{o}C/min.

2.4.3 Synthesis of Homo- and Copolymers

In a typical experiment (entry 2, Table 3), in a N_2 filled glove box, a glass-lined Parr high-pressure reactor was charged with chlorobenzene (5 ml), AIBN (0.005 g), MA (0.3 g), and Al_2O_3 (0.1775 g). The reactor was sealed, removed from glove box, and charged with ethene to 500 psi. The reaction mixture was allowed to stir in a 75 ^oC oil bath for 18 h. At the end of this period, the reactor was cooled and vented, and polymer was precipitated with a large excess of methanol. The polymer was collected by filtration and dried under high vacuum for 24 h. For those reactions, which did not require a Parr reactor, the polymerizations were carried out in 20 ml scintillation vials. The copolymer compositions were determined from ^{1}H-NMR integration of the methoxy protons versus aliphatic resonances.

2.4.4 Kinetic study of Methyl Acrylate and 1-Hexene Copolymerization

In a N_2 filled dry box, a reaction vessel with a magnetic bar was charged with chlorobenzene (20 mL), 1-hexene (3.0 g), methyl acrylate (0.9 g) and AIBN (0.015 g). The reaction vessel was then heated in an oil bath at 60 ^oC. Samples were taken with a syringe and used for GC analysis to determine the monomer conversions.

2.4.5 Synthesis of Copolymers with the Column Reactor

Typical column reactions were carried out in an Al_2O_3-filled column reactor (length, 100 cm; diameter, 20 cm; 35 g Al_2O_3) shown in Fig. 2. In a N_2 filled glove box, was added chlorobenzene (5 ml), AIBN (0.02 g), MA (1.0 g), and 1-hexene (3.0 g) to the Al_2O_3-filled column. The column was then sealed and removed from glove box. The reactor was then wrapped with a heating tape and heated to 60 ^oC and for 18 h. At the end of this period, the column was

cooled and washed with 300 ml of chloroform. The polymer solution was collected, concentrated and finally dried for 24 h to give the solid copolymer product. The column reactor was dried under N_2 flow for 24 h and reused for next polymerization.

2.5 References

1. Boffa, L. S.; Novak, B. M. *Chem. Rev.* **2000**, *100*, 1479-1493.

2. Ittel, S. D; Johnson, L. K.; Brookhart, M. *Chem. Rev.* **2000**, *100*, 1169-1204.

3. Liu, S.; Sen, A . *J. Polym. Sci., Part A: Polym. Chem.* **2004**, *42*, 6175-6192.

4. Liu, S.; Elyashiv, S.; Sen, A *J. Am. Chem. Soc.* **2001**, *123*, 12738-12739.

5. Elia, C.; Elyashiv, S.; Sen. A; Lopez-Fernandez, R; Albeniz, A. C.; Espinet, P. *Organomettallics* **2002**, *21*, 4249-4256.

6. Gu, B.; Liu, S.; Leber, D.; Sen, A. *Macromolecules* **2004**, *37*, 5142-5144.

7. Liu, S.; Gu, B.; Rowlands, H. A.; Sen, A. *Macromolecules* **2004**, *37*, 7924-7929.

8. Borkar, A.; Sen, A. *Macromolecules* **2005**, *38*, 3029-3032.

9. Nagel, M.; Poli, D.; Sen, A. *Macromolecules* **2005**, *38*, 7262-7265.

10. Tian, G. L.; Boone, H. W.; Novak, B. M. *Macromolecules* **2001**, *34*, 7656- 7663.

11. Venkatesh, R.; Klumperman, B. *Macromolecules* **2004**, *37*, 1226-1233.

12. Venkatesh, R.; Harrison, S.; Haddleton, D. M.; Klumperman, B. *Macromolecules* **2004**, *37*, 4406-4416.

13. Lutz, J. F.; Kirci, B.; Matyjaszewski, K. . *Macromolecules* **2003**, *36*, 3136-3145.

14. Isobe, Y.; Nakano, T.; Okamoto, Y. *J. Polym. Sci., Part A: Polym. Chem.* **2001**, *39*, 1463-1471.

15. Lutz, J. F.; Jakubowski, W.; Matyjaszewski, K. *Macromol. Rapid Comm.* **2004**, *25*, 486-492.

16. Ray, B.; Isobe, Y.; Matsumoto, K.; Habaue, S.; Okamato, Y. Kamigaito, M.; Sawamoto, M. *Macromolecules* **2004**, *37*, 1702-1710.

17. Logothetis, A. L.; McKenna J. M. *J. Polym. Sci., Polym. Chem. Ed.* **1977**, *15*, 1431-1439.

18. Logothetis, A. L.; McKenna J. M. *J. Polym. Sci., Polym. Chem. Ed.* **1978**, *16*, 2797-2802.

19. Gladysz, J. A. *Chem. Review* **2002**, *102*, 3215-3126.

Chapter 3

Rate Enhancement in Controlled Radical Polymerization of Acrylates Using Recyclable Heterogeneous Lewis Acid

3.1 Introduction

The growing demand for functionalized, structurally well-defined, polymeric materials has been a driving force for the development of controlled ("living") radical polymerization (CRP) techniques,[1] two notable examples of which are nitroxide-mediated polymerization (NMP)[2-5] and reversible addition-fragmentation transfer (RAFT) polymerization.[5-10] However, in order to have good control over the polymerization, the concentration of propagating radicals must be kept low to minimize bimolecular termination reactions. The price paid for this is the slow polymerization rate, which diminishes the practical utility of such systems. Clearly, strategies must be developed that allow CRP to be conducted at lower temperatures, in shorter time periods, and with higher monomer conversions.

One approach to increasing the radical polymerization rate of acrylate monomers is to use a Lewis acid as a complexation agent. The Lewis acid coordinates to the ester carbonyl group of the acrylate monomer and reduces the electron density in the conjugated C=C bond, thereby increasing the reactivity of the radical generated. Although rate acceleration in acrylate polymerizations by added Lewis acids has been previously reported, most Lewis acids employed thus far are relatively expensive materials that are soluble in the reaction medium and, therefore, not easily recycled.[11-16] From the standpoint of practical "Green Chemistry," the ideal Lewis acid should be insoluble and can be separated by filtration and reused. At first glance, this appears to

be a difficult problem because the radical polymerization would be expected to occur in the liquid monomer phase and the insoluble Lewis acid would be expected to have a minimal influence on the polymerization. However, as discussed above, the bonding of the acrylate monomer to the Lewis acid significantly increases the reactivity of radical. Thus, under ideal conditions, the acrylate monomer units that participate in the polymerization would be predominantly those that are bound to the heterogeneous Lewis acid. We obtained significant rate enhancement in NMP and RAFT polymerizations in the presence of a catalytic amount of solid acidic alumina (Al_2O_3) as Lewis acid. The acidic alumina can be recycled repeatedly without loss of activity.

3.2 Results and Discussion

3.2.1 Nitroxide Mediated Polymerization in the Presence of Acidic Alumina

The first-order plots in Figure **3-1** illustrate the rate enhancement in the presence of Lewis acids for the polymerization of n-butyl acrylate. While the rate enhancement was much higher in the presence of soluble $Sc(OTf)_3$, a significant deviation from linearity was observed at longer reaction times and the polydispersity (PDI) of the resultant polymers was high (2.3-3.6). Meanwhile the polymerization was well-behaved in the presence of acidic alumina (Aldrich, acidic, Brockmann I, standard grade, ~ 150 mesh, pH = 4.5±0.5 in aqueous solution) and proceeded at a rate (k_{obs}) significantly faster than that without the Lewis acid. Furthermore, the polymerization rate (k_{obs}) increased with increasing amount of added alumina (Figure **3-2**). The polydispersity of the polymers obtained in the presence of alumina remained low in every case (1.10-1.15). Figure **3-3** indicates that the polymerization is well-controlled and that alumina was

increasing the reactivity of the propagating radicals rather than promoting a fast exchange between radicals and their dormant species (which would result in a non-living process). In contrast to the observation with n-butyl acrylate, the rate (k_{obs}) of NMP-mediated polymerization of styrene, a monomer that cannot coordinate to a Lewis acid, was nearly unaffected by the addition of alumina (Figure **3-4**). This latter observation also suggests that there is no change in propagating radical concentration through the interaction of alumina with NMP.

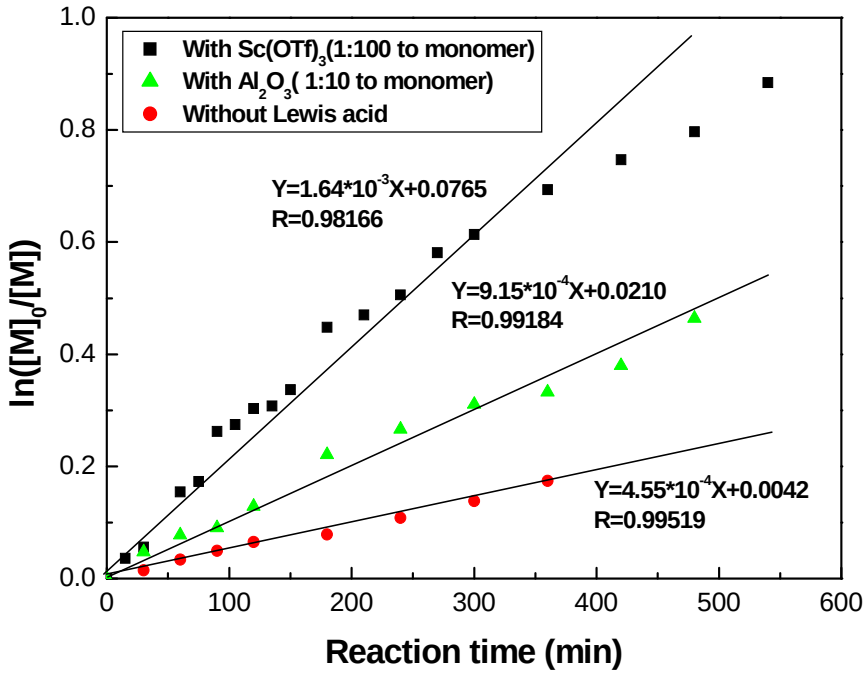

Figure **3-1**: Polymerisation kinetics for n-butyl acrylate (BA) in the presence and absence of Lewis acids ($Sc(OTf)_3$, 1 mol%; Al_2O_3, 10 mol%). Conditions: NMP initiator (2,2,5-trimethyl-3-(1-phenylethoxy)-4-phenyl-3-azahexane), 0.6 mmol; NMP control agent (2,2,5-trimethyl-4-phenyl-3-azahexane-3-nitroxide), 0.03 mmol; BA, 75 mmol; TCE, 0.5 g; PhCl, 20 mL; 125^{o}C.

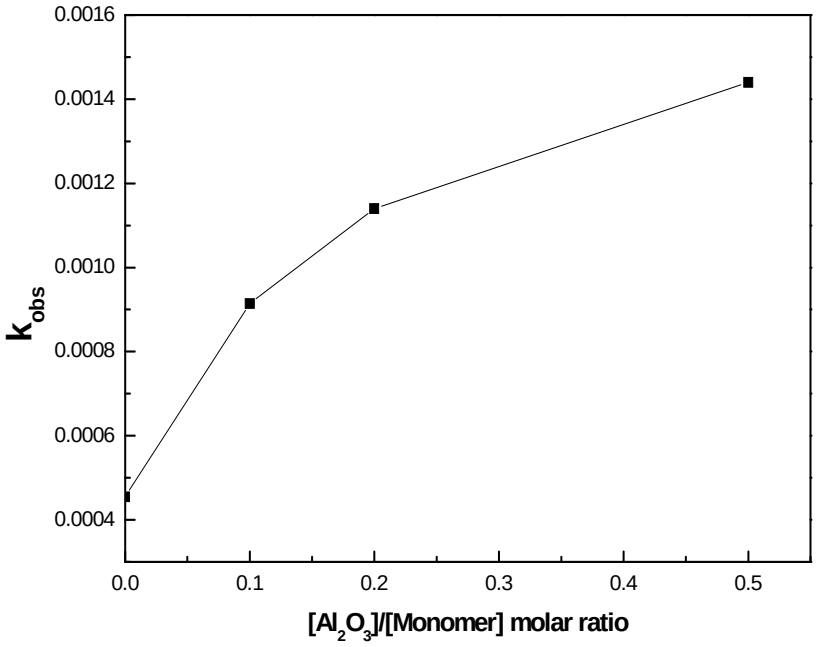

Figure **3-2**: Dependence of observed n-butyl acrylate polymerization rate on $[Al_2O_3]$/ [monomer] molar ratio. Conditions: NMP initiator (2,2,5-trimethyl-3-(1-phenylethoxy)-4-phenyl-3-azahexane), 0.6 mmol; NMP control agent (2,2,5-trimethyl-4-phenyl-3-azahexane-3-nitroxide), 0.03 mmol; BA, 75 mmol; Tetrachloroethane (TCE), 0.5 g; PhCl, 20 mL; 125^{o}C.

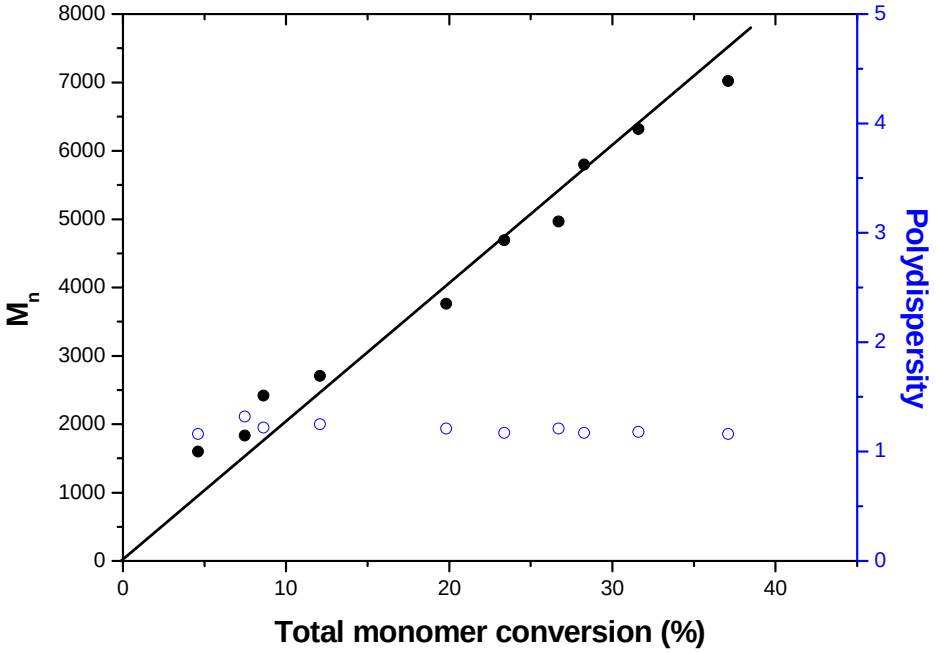

Figure **3-3**: Molecular weight and polydispersity dependence on total monomer conversion. Conditions: 10 mol % Al_2O_3, NMP initiator (2,2,5-trimethyl-3-(1-phenylethoxy)-4-phenyl-3-azahexane), 0.6 mmol; NMP control agent (2,2,5-trimethyl-4-phenyl-3-azahexane-3-nitroxide), 0.03 mmol; BA, 75 mmol; TCE, 0.5 g; PhCl, 20 mL; 125 ^{o}C.

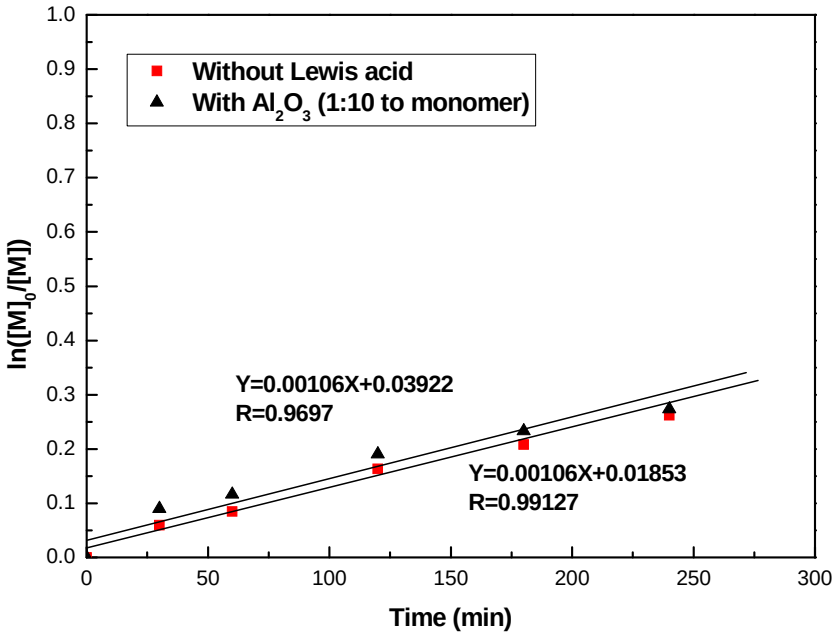

Figure **3-4**: Kinetics study of nitroxide mediated homopolymerization of styrene in the presence and absence of Lewis acid. Conditions: NMP initiator (2,2,5-trimethyl-3-(1-phenylethoxy)-4-phenyl-3-azahexane), 0.3 mmol; NMP control agent (2,2,5-trimethyl-4-phenyl-3-azahexane-3-nitroxide), 0.015 mmol; Styrene, 38 mmol; Tetrachloroethane (TCE), 0.5 g; PhCl, 10 mL; 125 ^{o}C.

The living nature of the n-butyl acrylate (BA) polymerization in the presence of alumina is further illustrated by the close correspondence between the theoretical molecular weight based on monomer/initiator ratio and the observed molecular weight. This is shown in Figure **3-5**; all of the PDI values were below 1.15.

More importantly, the nitroxide-terminated polymers made from these systems can be retreated with a different monomer for chain extension to form block copolymers. For example, an alkoxyamine functionalized poly(n-butyl acrylate) block (0.5 g; M_n, 15,000; PDI, 1.11) was initially grown in the presence of 10 mol% alumina and the resultant macroinitiator was employed to polymerize styrene (1.5 g) at 125^{o}C under N_2 for 8 h. This resulted in 61% conversion of styrene and gave a block copolymer, GPC analysis of which revealed the expected increased molecular weight (M_n, 55,000; PDI, 1.16) and no detectable amount of unreacted starting block (Figure **3-6**).

Finally, the alumina used for accelerating the NMP reactions can be readily removed by simple filtration and reused. As an example, the same sample of alumina was used for 5 successive n-butyl acrylate homopolymerizations. Typically, 96-98% of the alumina was recovered and for each polymerization cycle there was good agreement between theoretical and experimental M_n values (Table **3-1**) and the polydispersity remained below 1.15.

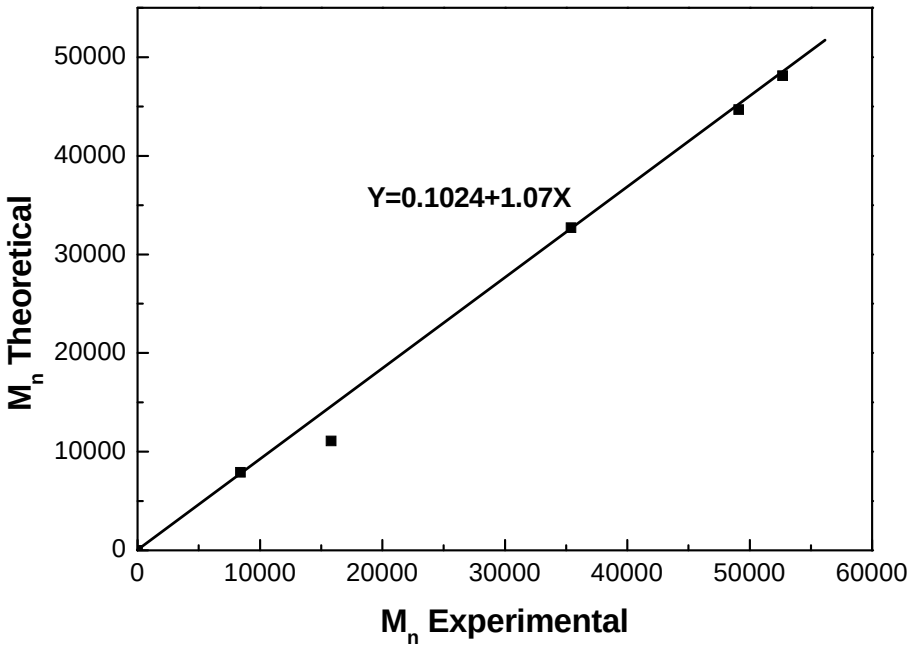

Figure **3-5**: Relationship between experimental molecular weight and theoretical molecular weight for the NMP of n-butyl acrylate in the presence of alumina (10 mol% relative to monomer). Conditions: NMP initiator (2,2,5-trimethyl-3-(1-phenylethoxy)-4-phenyl-3-azahexane), 1.0 equiv; NMP control agent (2,2,5-trimethyl-4-phenyl-3-azahexane-3-nitroxide), 0.05 equiv; 125 ^{o}C.

Table **3-1**: Nitroxide-mediated polymerisation (NMP) of n-butyl acrylate in the presence of acidic Al_2O_3[a].

Entry	[M] (g)	[M]/[I]	BA Conv. (%)	M_n expt. (x 10^{-4})[b]	M_n theo. (x 10^{-4})	PDI (M_w/M_n)[b]	Recycled Al_2O_3 (%)
1	12.8	1500	25	5.27	4.81	1.11	98
2	9.6	1125	31	4.91	4.47	1.14	99
3	6.4	750	34	3.54	3.27	1.15	99
4[c]	6.4	250	47	1.70	1.51	1.16	97
5	3.2	375	23	1.58	1.11	1.13	96
6[c]	3.2	125	59	1.10	0.95	1.15	95
7	1.6	188	33	0.84	0.79	1.15	98

[a]Conditions: Al_2O_3, 1:10(mol ratio) to monomer; NMP initiator(2,2,5-trimethyl-3-(1-phenylethoxy)-4-phenyl-3-azahexane) :22 mg NMP Control agent(2,2,5-trimethyl-4-phenyl-3-azahexane-3-nitroxide): 2mg; 125 ^{o}C,18 h. [b]By GPC (THF) relative to polystyrene standards. [c]Runs that using recycled Al_2O_3, NMP initiator(2,2,5-trimethyl-3-(1-phenylethoxy)-4-phenyl-3-azahexane) :65 mg NMP Control agent(2,2,5-trimethyl-4-phenyl-3-azahexane-3-nitroxide): 2 mg.

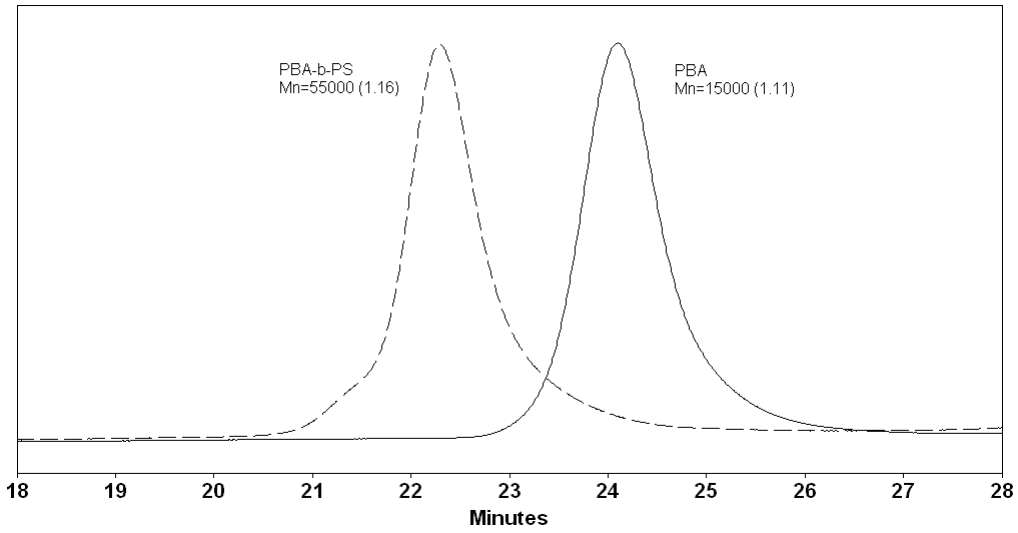

Figure **3-6**: GPC traces for the starting poly(n-butyl acrylate) made by NMP in the presence of alumina (left), and the poly(n-butyl acrylate)-b-polystyrene obtained after chain extension with styrene.

3.2.2 RAFT Polymerization in the Presence of Acidic Alumina

Figures **3-7** and **3-8** summarize our results on RAFT homopolymerization of methyl acrylate (MA) in the presence and absence of added alumina (10 mol% relative to monomer). A 5-fold increase in rate (k_{obs}) is observed in the presence of alumina. Furthermore, the linear relationship between molecular weight evolution and total monomer conversion and the narrow polydispersities (shown in Figure **3-8**) are consistent with a polymerization that is "living."

Table **3-2** summarizes the RAFT copolymerization of MA with 1-hexene. The copolymer compositions were determined from ^{1}H-NMR integration of the methoxy hydrogens versus total aliphatic hydrogens. Irrespective of the reaction conditions, it is clear that the conversion increases dramatically upon the addition of alumina. However, the polydispersity values for the copolymers are invariably higher than that observed with methyl acrylate homopolymers. One reason may be the coupling of the intermediate RAFT radical and the relatively unstable secondary radical derived from the 1-alkene. This process would be expected to be irreversible, leading to higher polydispersity.[5,10]

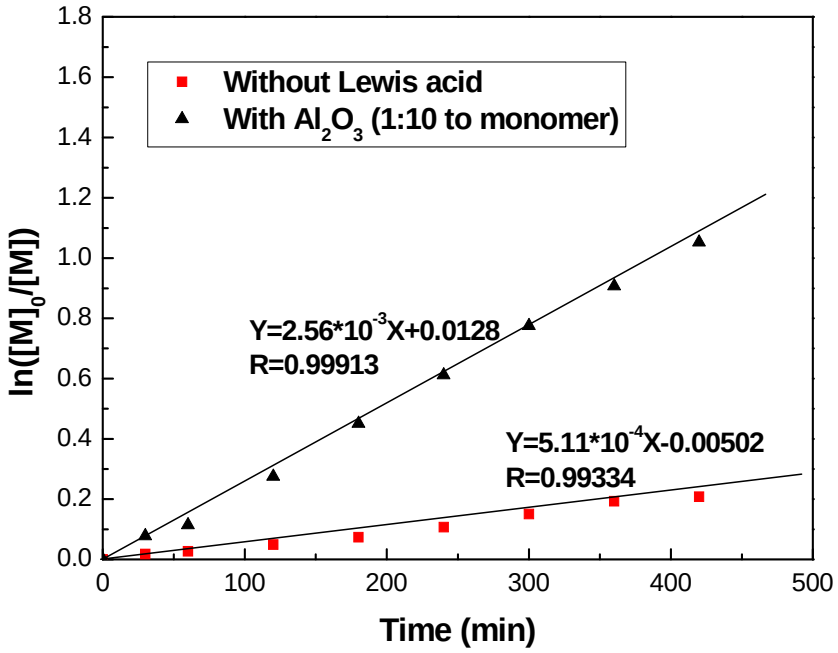

Figure **3-7**: Polymerization kinetics for methyl acrylate (MA=monomer) in the presence and absence of acidic alumina (10 mol% relative to MA). Conditions: reversible addition-fragmentation transfer (RAFT) (benzyl 1-pyrrol carbodithioate), 0.29 mmol; AIBN, 0.058 mmol; MA, 23.3 mmol; 60 ^{o}C.

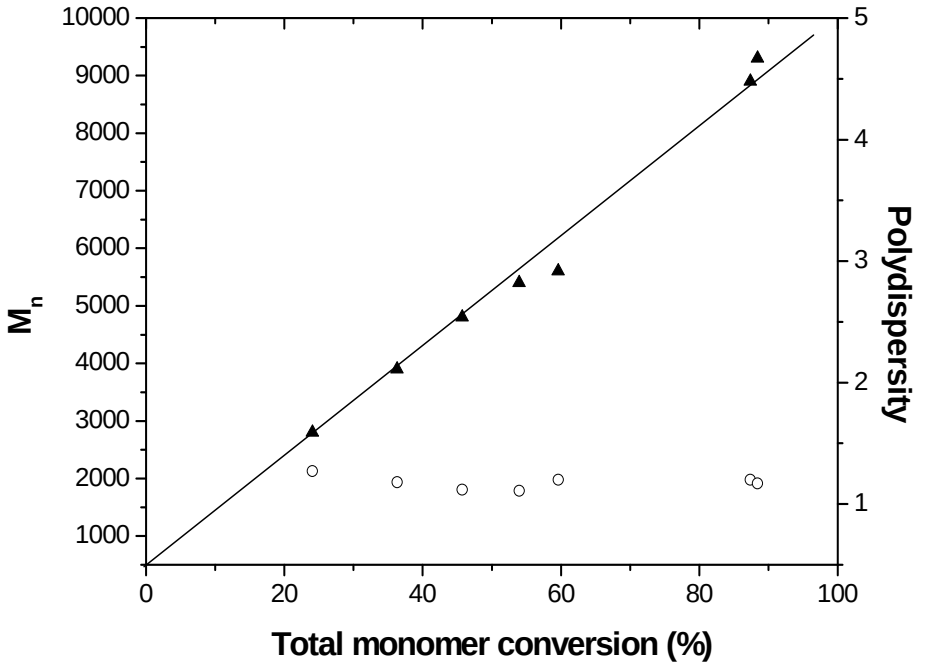

Figure **3-8**: Dependence of molecular weight and polydispersity on total monomer conversion for the RAFT homopolymerization of methyl acrylate (MA=monomer) in the presence of Al_2O_3 (10 mol% relative to MA). Conditions: RAFT (benzyl 1-pyrrolcarbodithioate), 0.29 mmol; 2, 2'-Azobis(isobutyronitrile) (AIBN), 0.058 mmol; MA, 23.3 mmol; Al_2O_3, 2.3 mmol; 60 ^oC.

Table **3-2**: Copolymerization of MA and 1-hexene with RAFT agent in batch reactions[a].

$[Al_2O_3]$/ [MA]	[RAFT]/ [AIBN]	Yield (g)	MA Conv. (%)	1-Hexene Incorp. (%)[b]	M_n (x 10^{-4})[c]	PDI (M_w/M_n)[c]
0	5	1.09	41.4	8.6	0.87	1.61
1:10	5	2.21	80.4	12.8	1.06	1.56
0	10	1.01	38.0	10.0	0.53	1.48
1:10	10	1.27	59.1	10.3	0.69	1.46

[a]Conditions: MA, 2.4 g; 1-Hexene, 1.5 g; AIBN, 6 mg; PhCl, 5 ml; 60 ^{o}C,18 h. [b]By ^{1}H-NMR spectroscopy.
[c]By GPC (THF) relative to polystyrene standards.

3.3 Conclusion

In summary, the addition of insoluble acidic alumina to controlled radical NMP and RAFT polymerizations of acrylate monomers results in significantly higher reaction rates and conversions. Parallel experiments with monomers that can and cannot interact with the Lewis acid suggest that the observed effect is not due to a change in the concentration of propagating radicals in the system. The accelerating effect is particularly dramatic since only a small fraction of the Lewis acid sites that are present on the alumina surface can actually interact with the acrylate. Preliminary NMR studies on the coordination of soluble Lewis acids to the ester carbonyl of acrylate monomers and polymers suggest that the interaction with the monomer is significantly stronger than that with the polymer,[14] thus explaining why only a catalytic amount of Lewis acid is required for polymerization rate enhancement. The Lewis acid-enhanced polymerizations have "living" characteristics, allowing the synthesis of block copolymers. The alumina can be quantitatively removed by filtration and recycled with no significant loss in efficacy.

3.4 Experimental Procedures

3.4.1 Materials

All chemicals and reagents were obtained from Aldrich unless otherwise stated. Methyl acrylate (MA, 99%), n-butyl acrylate (BA, 99%), and 1-hexene were vacuum distilled from CaH_2 and stored under N_2. 2, 2'-Azobis(isobutyronitrile) (AIBN, 98%), aluminum oxide (activated, acidic, Brockmann I, standard grade, ~ 150 mesh, pH = 4.5± 0.5 in aqueous solution), and scandium triflate ($Sc(OTf)_3$, 98%) was used as received.

The NMP initiator, 2, 2, 5- trimethyl- 3- (1-phenylethoxy)-4-phenyl-3-azahexane, and the NMP control agent, 2, 2, 5- trimethyl-4-phenyl-3-azahexane-3-nitroxide, were synthesized and purified following literature procedure [Benoit, D.; Chaplinski, V.; Braslau, R.; Hawker, C. J. *J. Am. Chem. Soc.* **1999**, *121*, 3904-3920]. The RAFT agent, benzyl 1-pyrrolcarbodithioate was synthesized and purified following literature procedure [Chiefari, J.; Mayadunne, R. T. A.; Moad, C. L.; Moad, G.; Rizzardo, E.; Postma, A.; Skidmore, M. A.; Thang, S. H. *Macromolecules* **2003**, *36*, 2273-2283].

3.4.2 Instrumentation

^{1}H- and ^{13}C-NMR spectra were recorded using a Bruker 300-DPX spectrometer at ambient temperature (^{1}H-NMR, 300MHz; ^{13}C-NMR, 75 MHz). Chemical shifts are referenced to $CDCl_3$. Molecular weights and polydispersities were determined on a Shimadzu gel permeation chromatography (GPC) chromatograph containing a three-column bed (styragel HR 7.8 × 300 mm columns with 5 μm beads size; 100-5000, 500-30,000, and 2,000-4 × 10^6 Da), a Shimadzu

RDI-10A differential refractometer, and a Shimadzu SPD-10A tunable absorbance detector (254 nm). GPC samples were run in tetrahydrofuran at a flow rate of 1 ml/min at 35 ^{o}C and calibrated against polystyrene standards. Analysis was done using EZSTART 7.2 software. Gas chromatography(GC) analysis was performed on an Agilent 5890 Series II GC. The samples were heated from 40 ^{o}C to 100 ^{o}C at a ramp rate of 4 ^{o}C/min.

3.4.3 Kinetic Study of Nitroxide Mediated Polymerization of n-Butyl Acrylate in the Presence and Absence of Acidic Alumina

In a N_2-filled dry box, a round bottom flask equipped with a magnetic stir bar was charged with NMP initiator (195 mg, 1.0 equiv.), NMP control agent (6 mg, 0.05 equiv.), BA (9.6 g, 125 equiv.), internal standard tetrachloroethane (TCE, 0.5 g), acidic alumina (0.765 g, 1:10 to monomer) and chlorobenzene (20 ml). The flask was then placed in an oil bath at 125^{o}C. Samples were taken at specific time intervals using a syringe and analyzed by GC. The conversion of BA was calculated from the integration of BA peak with respect to TCE peak. The molecular weight was measured by GPC.

3.4.4 General Procedure for Nitroxide Mediated Polymerization of n-Butyl Acrylate in the Presence of Acidic Alumina

In a N_2-filled dry box, a mixture of NMP initiator (33 mg, 1.0 equiv.), NMP control agent (1 mg, 0.05 equiv.), BA (3.2 g, 250 equiv.), acidic alumina (0.255 g, 1:10 to monomer) and chlorobenzene (5 ml) was sealed in 20 ml scintillation vial. The reaction mixture was allowed to stir in a 125 ^{o}C oil bath for 18 h. At the end of this period, the alumina was removed by filtration, and the polymer was precipitated with a large excess of methanol. The polymer was collected by filtration and dried under high vacuum for 24 h.

3.4.5 Kinetic Study of Nitroxide Mediated Polymerization of Styrene in the Presence and Absence of Acidic Alumina

In a N_2-filled dry box, a round bottom flask equipped with a magnetic stir bar was charged with NMP initiator (98 mg, 1.0 equiv.), NMP control agent (3 mg, 0.05 equiv.), styrene (3.9 g, 125 equiv.), internal standard tetrachloroethane (TCE, 0.5 g), acidic alumina (0.382 g, 1:10 to monomer) and chlorobenzene (10 ml). The flask was then placed in an oil bath at 125^{o}C. Samples were taken at specific time intervals using a syringe and analyzed by GC. The conversion of styrene was calculated from the integration of styrene peak with respect to TCE peak. The molecular weight was measured by GPC.

3.4.6 General Procedure for Block Copolymer Formation: Preparation of Poly(n-Butyl Acrylate)-b- Polystyrene

In a N_2-filled dry box, a mixture of NMP initiator (33 mg, 1.0 equiv.), NMP control agent (1 mg, 0.05 equiv.), BA (3.2 g, 250 equiv.), acidic alumina (0.255 g, 1:10 to monomer) and chlorobenzene (5 ml) was sealed in 20 ml scintillation vial. The reaction mixture was allowed to stir in a 125 ^{o}C oil bath for 18 h. At the end of this period, the polymer was precipitated with a large excess of methanol. The colorless polymer was collected by filtration and dried under high vacuum for 24 h. The poly(n-butyl acrylate), starting block (M_n=15000, PDI= 1.11, 0.5 g, 0.033 mmol) was then redissloved in styrene (1.5 g, 14.4 mmol), and the mixture was heated at 125 ^{o}C for 8 h. The solidified reaction mixture was dissolved in dichloromethane and precipitated into methanol. The polymer was collected by filtration and dried under high vacuum for 24 h to give the desired diblock copolymer as a white solid (1.41g, 61%), M_n, 55000; PDI, 1.16.

3.4.7 Kinetic Study of RAFT Polymerization of Methyl Acrylate in the Presence and Absence of Acidic Alumina

In a N_2-filled dry box, a round bottom flask equipped with a magnetic stir bar was charged with MA (2.0 g, 23.3 mmol), benzyl 1-pyrrocarbodithioate (0.068 g, 0.29 mmol), AIBN (9.5 mg, 0.058 mmol), internal standard tetrachloroethane (TCE, 0.5 g), acidic alumina (0.237 g, 1:10 to monomer) and chlorobenzene (15 ml). The flask was then placed in an oil bath at 60^{o}C. Samples were taken at specific time intervals using a syringe and analyzed by GC. The conversion of MA was calculated from the integration of MA peak with respect to TCE peak. The molecular weight was measured by GPC.

3.5 References

1. Matyjaszewski, K.; Ed. Advances in Controlled/ Living Radical Polymerization; American Chemical Society: Washington, DC, 2003; Vol. 854.

2. Hawker, C. J.; Bosman, A. W.; Harth, E. *Chem. Rev.* **2001**, *101*, 3661-3688.

3. Benoit, D.; Chaplinski, V.; Braslau, R.; Hawker, C. J. *J. Am. Chem. Soc.* **1999**, *121*, 3904-3920.

4. Gu, B.; Liu, S.; Leber, D.; Sen, A. *Macromolecules* **2004**, *37*, 5142-5144.

5. Liu, S.; Sen, A . *J. Polym. Sci., Part A: Polym. Chem.* **2004**, *42*, 6175-6192.

6. Chong, Y. K.; Kristina, J.; Le, T. P. L.; Moad, G.; Postma, A.; Rizzardo, E.; Thang, S. H. *Macromolecules* **2003**, *36*, 2256-2272.

7. Chiefari, J.; Mayadunne, R. T. A.; Moad, C. L.; Moad, G.; Rizzardo, E.; Postma, A.; Skidmore, M. A.; Thang, S. H. *Macromolecules* **2003**, *36*, 2273-2283.

8. Mayadunne, R. T. A.; Rizzardo, E.; Chiefari, J.; Chong, Y. K.; Moad, G.; Thang, S. H. *Macromolecules* **1999**, *32*, 6977-6980.

9. Chiefari, J.; Chong, Y. K.; Ercole, F.; Kristina, J.; Jeffery, J.; Le, T. P. L.; Mayadunne, R. T. A.; Meijs, G. F.; Moad, C. L.; Moad, G.; Rizzardo, E.; Thang, S. H. *Macromolecules* **1998**, *31*, 5559-5562.

10. Liu, S.; Gu, B.; Rowlands, H. A.; Sen, A. *Macromolecules* **2004**, *37*, 7924-7929.

11. Lutz, J. F.; Neugebauer, D.; Matyjaszewski, K. *J. Am. Chem. Soc.* **2003**, *125*, 6986-6993.

12. Lutz, J. F.; Kirci, B.; Matyjaszewski, K. *Macromolecules* **2003**, *36*, 3136-3145.

13. Lutz, J. F.; Jakubowski, W.; Matyjaszewski, K. *Macromol. Rapid Comm.* **2004**, *25*, 486-492.

14. Isobe, Y.; Nakano, T.; Okamoto, Y. *J. Polym. Sci., Part A: Polym. Chem.* **2001**, *39*, 1463-1471.

15. Ray, B.; Isobe, Y.; Matsumoto, K.; Habaue, S.; Okamato, Y. Kamigaito, M.; Sawamoto, M. *Macromolecules* **2004**, *37*, 1702-1710.

16. Nagel, M.; Poli, D.; Sen, A. *Macromolecules* **2005**, *38*, 7262-7265.

Chapter 4

Effects of Lewis and Brønsted Acids on the Homopolymerization of Acrylates and Their Copolymerization with 1-Alkenes

4.1 Introduction

The copolymers of polar acrylate monomers with simple 1-alkenes with predictable composition and architectures have attracted great interest because the combination of these two classes of monomers can greatly enhances the currently attainable polymer properties.[1-3] However, because of the wide disparity between the respective reactivity ratios, random acrylate-rich copolymers in relatively low yields are typically obtained by free radical copolymerization of the two.[4-12] We have recently reported that free radical copolymerization of acrylate with simple 1-alkenes in the presence of a recyclable heterogeneous Lewis acids, alumina, can lead to a significant increase in the polymerization rate and non-polar alkene incorporation.[13,14] The rationale is that Lewis acids can coordinate with the carbonyl group of the acrylate monomer and reduce the electron density of the conjugated double bond, thereby increasing the reactivity of the acrylate radical and making the radical more susceptible to attack by the relatively electron rich non-polar alkene.[15-20] Besides Lewis acids, a strong organic Brønsted acid has also been used in the copolymerization of acrylonitrile with ethene.[21]

We investigated the first copolymerization of acrylate and methacrylate with non-polar 1-alkenes in the presence of recyclable heterogeneous Brønsted acids as complexation agents. The use of either homogeneous (pyridinium triflate (PyH)) or heterogeneous Brønsted acid (crosslinked poly(4-vinylpyridinium p-toluenesulfonate) (PPyH) and Nafion) resulted in the copolymerizations proceeding with higher conversion and increased 1-alkene incorporation.

Further, the heterogeneous Brønsted acids can be recycled repeatedly without attenuation of activity.

We also examined the relationship between the complexing ability of the Lewis and Brønsted acids vis-à-vis the carbonyl group of the ester functionality and their ability to promote acrylate and methacrylate homo and copolymerizations and we find a direct correlation between the two. Likewise, for soluble Lewis acids, there is a direct correlation between the charge/size ratio at the metal center their ability to promote copolymerizations. Thus, our study provides a semi-quantitative ways of estimating the efficacy of a given Lewis or Brønsted acid in promoting acrylate/methacrylate polymerizations.

4.2 Results and Discussion

4.2.1 Brønsted Acid- Mediated Copolymerization of Methyl Acrylate and 1-Alkenes

The effect of adding pyridinium triflate (PyH) to the AIBN-initiated copolymerization of methyl acrylate (MA) with 1-alkenes was examined and the results are summarized in Table **4-1**. The copolymer compositions were determined by ^{1}H NMR integration of the methoxy proton vs. aliphatic protons. Upon adding PyH, both 1-alkene incorporation and, especially, the copolymer yield increases. In all cases, it was confirmed by gel permeation chromatography (GPC) that these were true copolymers instead of mixtures of homopolymers. The GPC chromatograms showed only one peak with both refractive index (RI) and UV detector. The latter is more sensitive to acrylate monomers. This indicates a true copolymer over the entire molecular weight distribution range. The copolymer microstructure was examined by ^{1}H and ^{13}C-NMR spectroscopy. The ^{13}C NMR spectrum of a typical MA and ethene copolymer (e.g. entry 2, Table **4-1**) showed five major resonances at 175.8 (-C(O)-), 51.6 (-OCH_3), 45.1 (-CH-), 32.9 (-CH_2-), 25.5 (-CH_2-) ppm

for the alternating MA-ethene copolymer sequence. Less intense peaks were observed at 43.1 and 34.6 ppm attributable to consecutive MA units and even lower intensity peaks at 29.3 and 27.2 ppm attributable to consecutive ethene units, suggesting a small degree of non-alternation.[7]

Table **4-1**: Copolymerization of MA with 1-alkenes in the presence and absence of pyridinium triflate (PyH)[a]

Entry	1-alkene (psi or g)	[Py]/[MA] (mol ratio)	Yield (g)	MA conv. (mol%)	Alkene incorp. (mol%)	Mn[b] (*10^{-4})	PDI[b]
1	Ethene (500)	0	0.085	24.5	31.6	2.84	1.57
2	Ethene (500)	1:5	0.170	48.7	33.6	2.00	1.61
3	Ethene (500)	1:2	0.174	49.3	35.1	1.90	1.75
5	1-hexene (1.0)	0	0.139	36.2	22.3	1.27	1.66
6	1-hexene (1.0)	1:5	0.239	60.0	25.1	0.92	1.89
7	1-hexene (1.0)	1:2	0.241	60.3	25.4	0.90	1.91

[a]Conditions: MA, 0.3 g; AIBN, 0.005 g; Toluene, 5 mL; 60 ^{o}C, 18 h. [b]By GPC using polystyrene standards.

Encouraged by the above results with a homogeneous Brønsted acid, we next examined the effect of heterogeneous Brønsted acid because of the ease of separation and recycling of the latter. Two commercially available heterogeneous Brønsted acids, poly(4-vinylpyridinium p-toluenesulfonate), PPyH, and Nafion, were employed as complexation agents. It was anticipated that hydrogen bonding, formed between the acrylate carbonyl group and the proton present on the surface of the insoluble Brønsted acid, will significantly increase the reactivity of the acrylate monomers. Under ideal conditions, the acrylate monomers that participate in the polymerization would predominantly be those that are hydrogen bonded to the surface of the heterogeneous Brønsted acid.

The copolymerization results of MA and 1-alkenes in the presence and absence of heterogeneous crosslinked polypyridinium polymer, PPyH, are summarized in Table **4-2**. Similar to the results of soluble pyridinium triflate, a significant increase in monomer conversion was observed upon the addition of PPyH irrespective of the alkene examined. Clearly even a Brønsted acid that is insoluble in the reaction medium can still enhance the reactivity of the propagating radical through surface hydrogen bonding. Furthermore, PPyH can be recovered by simple filtration and reused with no obvious attenuation of reactivity (entries 4 and 8 of Table **4-2**). Another commercially available proton acid, Nafion (SAC-13, strongly acidic catalyst resin, surface area > 200 m^2/g) was also employed in the copolymerizations of MA with 1-alkenes (Table **4-3**). Again a significant increase in monomer conversion was observed upon the addition of Nafion irrespective of the alkene examined. Nafion can also be recovered by filtration and reused (entries 4 and 8 of Table **4-3**).

Table **4-2**: Copolymerization of MA with 1-alkenes in the presence and absence of poly(4-vinylpyridinium p-toluenesulfonate), PPyH[a]

Entry	1-alkene (psi or g)	PPyH (g)	Yield (g)	MA Conv. (mol%)	Alkene incorp. (mol%)	Mn[c] (*10^{-4})	PDI[c]	PPyH Recycled (%)
1	Ethene (500)	0	0.085	24.5	31.6	2.84	1.57	-
2	Ethene (500)	0.1	0.178	50	36.3	3.89	1.69	94
3	Ethene (500)	0.2	0.188	51.4	39.9	3.73	1.68	92
4[b]	**Ethene (500)**	**0.1**	**0.176**	**50.1**	**34.6**	**1.92**	**1.75**	**97**
5	1-hexene (1.0)	0	0.139	36.2	22.3	1.27	1.66	-
6	1-hexene (1.0)	0.1	0.2056	52	24.4	0.99	2.10	89
7	1-hexene (1.0)	0.2	0.230	58	24.7	1.16	2.05	96
8[b]	**1-hexene (1.0)**	**0.1**	**0.261**	**64.3**	**26.6**	**0.97**	**1.85**	**93**

[a]Conditions: MA, 0.3 g; AIBN, 0.005 g; Toluene, 5 mL; 60 ^{o}C, 18 h. [b]By using recycled PPy. [c]By GPC using polystyrene standards.

Table **4-3**: Copolymerization of MA and 1-alkenes in the presence and absence of Nafion[a]

Entry	1-alkene (psi or g)	Nafion (g)	Yield (g)	MA Conv. (mol%)	Alkene incorp. (mol%)	Mn[c] (*10^{-4})	PDI[c]	Nafion Recycled (%)
1	Ethene (500)	0	0.084	24.5	31.6	2.84	1.57	-
2	Ethene (500)	0.2	0.193	57.2	34.9	1.84	2.06	87
3	Ethene (500)	0.4	0.201	56.2	30.8	1.93	1.69	90
4[b]	**Ethene (500)**	**0.4**	**0.198**	**55.3**	**37.4**	1.99	1.67	**90**
5	1-hexene (1.0)	0	0.139	36.2	22.3	1.27	1.66	-
6	1-hexene (1.0)	0.2	0.326	80.2	26.7	1.15	2.32	91
7	1-hexene (1.0)	0.4	0.328	80.0	27.4	1.02	1.73	90
8[b]	**1-hexene (1.0)**	**0.4**	**0.307**	**74.9**	**26.3**	**0.90**	**1.83**	**93**

[a]Conditions: MA, 0.3 g; AIBN, 0.005 g; Toluene, 5 mL; 60 ^{o}C, 18 h. [b]By using recycled Nafion. [c]By GPC using polystyrene standards.

4.2.2 Heterogeneous Brønsted Acid Mediated Copolymerization of Methyl Methacrylate and 1-Alkenes

Both PPyH and Nafion were also found effective in promoting the copolymerization of methyl methacrylate (MMA) and 1-alkenes as shown in Table **4-4** and **4-5**, respectively. The copolymer composition was determined through ^{1}H NMR integration of methoxy proton vs. aliphatic protons. A true copolymer over the entire molecular weight distribution range was confirmed by GPC using both UV and RI detectors. Irrespective of the 1-alkene employed, a dramatic increase (approximately 2-3 times higher) in monomer conversion was observed. Furthermore, both PPyH and Nafion can be recovered by simple filtration and reused with no obvious attenuation of reactivity (entries 4 and 8 of Table **4-4**, entries 4 and 8 of Table **4-5**).

Table **4-4**: Copolymerization of MMA and 1-alkenes in the presence and absence of PPyH[a]

Entry	1-alkene (psi or g)	PPyH (g)	Yield (g)	MMA Conv. (mol%)	Alkene incorp. (mol%)	Mn[c] (*10^{-4})	PDI[c]	PPyH Recycled (%)
1	Ethene (500)	0	0.044	13.7	18.2	1.68	2.39	-
2	Ethene (500)	0.05	0.137	42.4	22.0	2.18	1.47	92
3	Ethene (500)	0.1	0.145	44.8	22.0	1.87	2.02	98
4[b]	**Ethene (500)**	**0.1**	**0.153**	**47.0**	**23.3**	**3.24**	**1.99**	**89**
5	1-hexene (1.0)	0	0.103	32.2	7.6	2.35	1.50	-
6	1-hexene (1.0)	0.05	0.244	74.0	10.4	1.73	1.43	99
7	1-hexene (1.0)	0.1	0.250	74.7	12.2	1.44	1.53	94
8[b]	**1-hexene (1.0)**	**0.1**	**0.281**	**87.0**	**8.33**	**2.53**	**1.55**	**90**

[a]Conditions: MMA, 0.3 g; AIBN, 0.005 g; Toluene, 5 mL; 60 ^{o}C, 18 h. [b]By using recycled PPy. [c]By GPC using polystyrene standards.

Table **4-5**: Copolymerization of MMA and 1-alkenes in the presence and absence of Nafion[a]

Entry	1-alkene (psi or g)	Nafion (g)	Yield (g)	MMA Conv. (mol%)	Alkene Incorp. (mol%)	Mn[c] ($*10^{-4}$)	PDI[c]	Nafion Recycled (%)
1	Ethene (500)	0	0.044	13.7	18.2	1.68	2.39	-
2	Ethene (500)	0.2	0.165	50.8	22.9	2.95	1.45	90
3	Ethene (500)	0.4	0.199	60.3	25.7	2.23	1.80	99
4[b]	Ethene (500)	0.4	0.184	56.1	25.0	1.87	1.96	89
5	1-hexene (1.0)	0	0.103	32.2	7.6	2.35	1.50	-
6	1-hexene (1.0)	0.2	0.230	68.6	12.5	1.41	2.06	92
7	1-hexene (1.0)	0.4	0.221	65.2	13.5	1.33	1.59	94
8[b]	1-hexene (1.0)	0.4	0.257	76.4	12.4	1.25	1.85	97

[a]Conditions: MMA, 0.3 g; AIBN, 0.005 g; Toluene, 5 mL; 60 ^{o}C, 18 h. [b]By using recycled Nafion. [c]By GPC using polystyrene standards.

4.2.3 NMR Study of Acrylate Monomer-Acid Interaction: Effect of Acid Complexation Strength on Polymerization Rate

The above results on the beneficial effect of Brønsted acids on the copolymerization of acrylate and methacrylate with 1-alkenes, taken together with our previous study of a similar effect of Lewis acids (both homogeneous and heterogeneous) suggested a possible correlation between the strength of the interaction of the acid with the acrylate monomer and the promotional effect of the former in polymerizations. One way to probe the complexation of the acid with the acrylate ester functionality is to monitor the ^{13}C NMR chemical shift of the carbonyl group, the most likely binding site. Indeed, this carbon showed the biggest downfield shift upon the addition of an acid (Brønsted or Lewis) to the acrylate monomer. As postulated, this interaction of the acid with the ester carbonyl group will reduce the electron density of the conjugated double bond, thereby increasing the reactivity of the acrylate radical and making the radical more susceptible to attack by the relatively electron rich non-polar alkene.

The apparent polymerization rates for both MA homopolymerization and MA/1-hexene copolymerization are first-order with respect to MA concentration. A correlation of apparent MA homopolymerization rate (Figure **4-1** (a)) and MA-1-hexene copolymerization rate (Figure **4-1** (b)) vs. shift in the ^{13}C NMR resonance of the MA carbonyl group is shown for both Brønsted and Lewis acids. The effect of the catalyst amount on polymerization rate was also examined (Figure **4-2**). Both figures clearly indicate a strong correlation between the strength of the interaction of the acid (Brønsted or Lewis) with the acrylate carbonyl group and the acid's ability to promote acrylate/methacrylate homo and copolymerizations. For Lewis acids, the charge/size ratio at the metal center is another measure of their strength and again there is a strong direct correlation between the magnitude of this number and the ability of the Lewis acid to promote

copolymerizations (Figure **4-3**). These correlations serve as useful tools to evaluate the effectiveness of a given acid in promoting acrylate homo and copolymerizations.

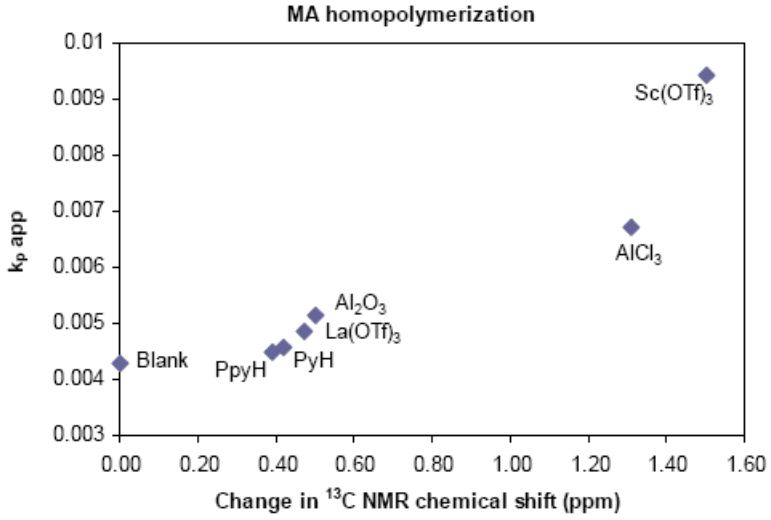

(a)

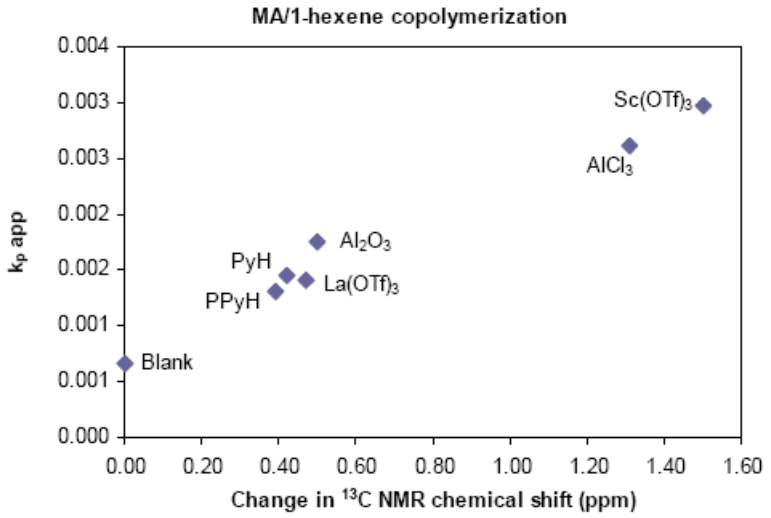

(b)

Figure **4-1**: (a) Homopolymerization rate vs. change in ^{13}C NMR chemical shift of the monomer carbonyl carbon. (b) Copolymerization rate vs. change in ^{13}C NMR chemical shift of the monomer carbonyl carbon. Conditions (a): MA, 0.6 g; AIBN, 5 mg; toluene, 5 mL; acids, 1:10 (molar ratio) to MA; 60 ^{o}C; 2 h. (b): MA, 0.3 g; 1-hexene, 1 g; AIBN, 5 mg; toluene, 5 mL; acids, 1:10 (molar ratio) to MA; 60 ^{o}C; 4 h.

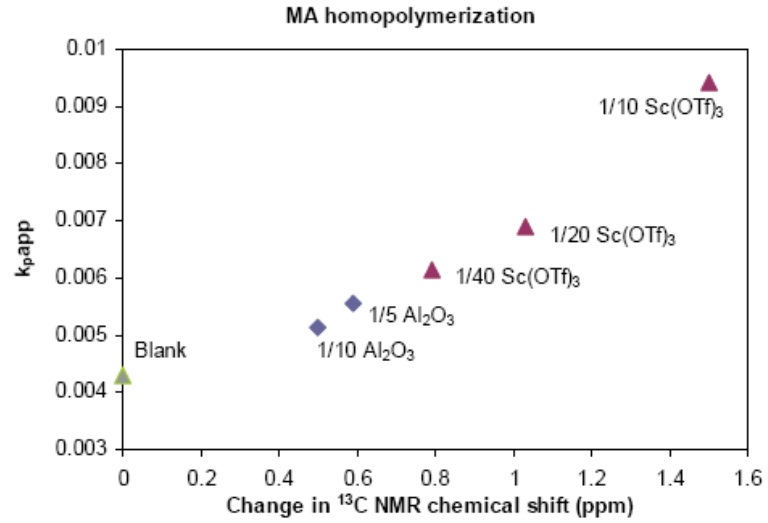

(a)

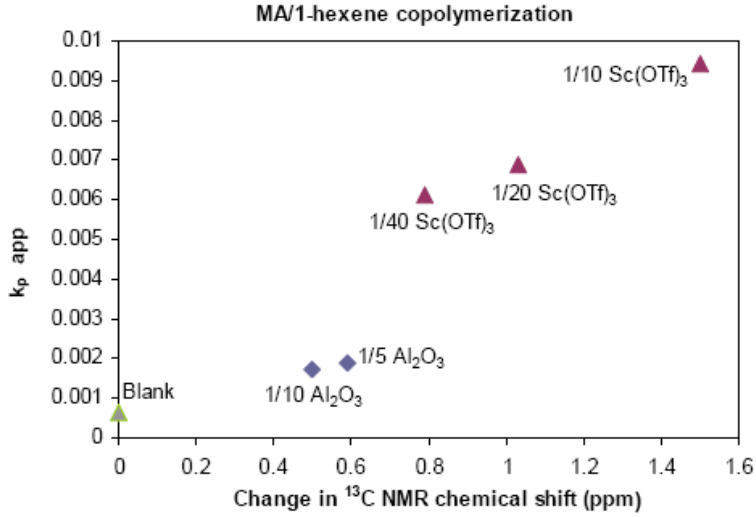

(b)

Figure **4-2**: (a) Homopolymerization rate vs. change in ^{13}C NMR chemical shift of the monomer carbonyl group for different catalyst/monomer molar ratios. (b) Copolymerization rate vs. change in ^{13}C NMR chemical shift of the monomer carbonyl carbon for different acid to monomer molar ratios. Conditions (a): MA, 0.6 g; AIBN, 5 mg; toluene, 5 mL; 60 ^{o}C; 2 h. (b): MA, 0.3 g; 1-hexene, 1 g; AIBN, 5 mg; toluene, 5 mL; 60 ^{o}C; 4 h.

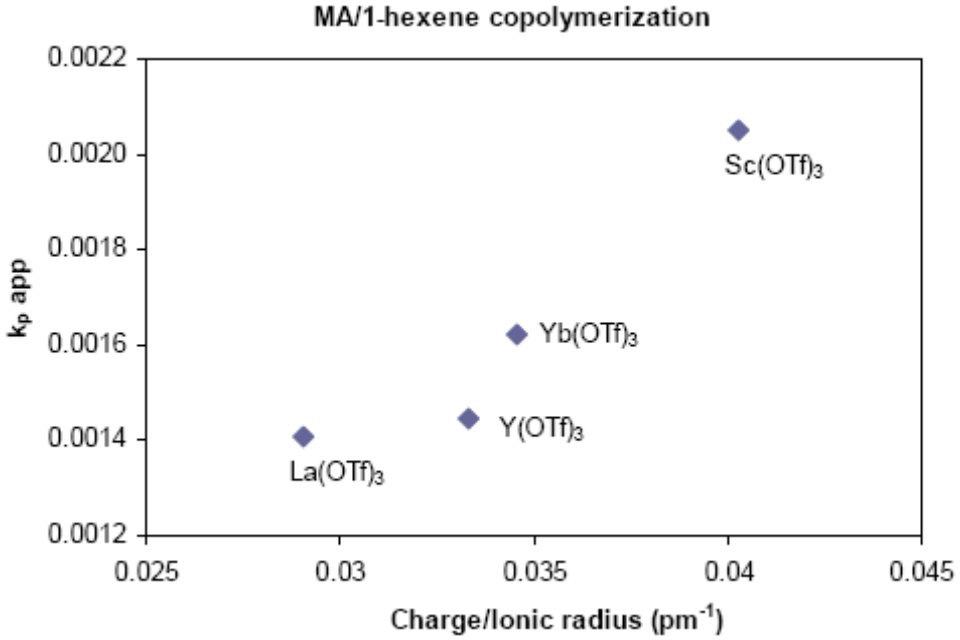

Figure **4-3**: MA/ 1-hexene copolymerization rate vs. charge/ionic radius ratio of the metal. Conditions: MA, 0.3 g; 1-hexene, 1 g; AIBN, 5 mg; toluene, 5 mL; $M(OTf)_3$/MA, 1:10 (molar ratio); 60 ^oC; 4 h.

4.3 Conclusion

The addition of either soluble or insoluble Brønsted acids to AIBN-initiated copolymerization of acrylate and methacrylate with non-polar alkenes resulted in increased monomer conversion and increased incorporation of the alkene into the polymer backbone. Studies indicate a strong correlation between the strength of the interaction of the acid (Brønsted or Lewis) with the acrylate carbonyl group and the acid's ability to promote acrylate/methacrylate homo and copolymerizations. This effect is particularly dramatic for insoluble acids since only a small fraction of the sites on the surface of the acid can actually interact with the ester functionality. The insoluble, heterogeneous, Brønsted acids can be recovered by simple filtration and reused without loss of activity.

4.4 Experimental Procedure

4.4.1 Materials

All chemicals and reagents were obtained from Aldrich unless otherwise stated. Methyl acrylate (MA, 99%), Methyl Methacrylate (MMA, 99%), 1-hexene (97%), were passed through basic alumina column to remove the inhibitor, degassed and stored under N_2. 2,2'-Azobis(isobutyronitrile) (AIBN, 98%), pyridinium trifluoromethanesulfonate(PyH, 97%), poly(4-vinylpyridinium p-toluenesulfonate) (PPyH, 2% crosslinked), Nafion SAC-13 (strongly acidic catalyst resin, pore diameter 10 nm; pore volume 0.6 mL/g; surface area > 200 m^2/g), lanthanum(III) trifluoromethanesulfonate ($La(OTf)_3$, 97%, Strem Chemicals), aluminum oxide (activated, acidic, Brockmann I, standard grade, ~ 150 mesh, pH = 4.5±0.5 in aqueous solution), aluminum chloride ($AlCl_3$, anhydrous, 99.99%), yttrium(III) trifluoromethanesulfonate ($Y(OTf)_3$, 98%), ytterbium(III) trifluoromethanesulfonate ($Yb(OTf)_3$, 97%) and scandium(III) trifluoromethanesulfonate ($Sc(OTf)_3$, Alfa Aesar, 98%) were used as received.

4.4.2 Instrumentation

NMR spectra were recorded using a Bruker 300-DPX spectrometer at ambient temperature (^{1}H-NMR, 300MHz; ^{13}C-NMR, 75 MHz). Chemical shifts are referenced to $CDCl_3$. Molecular weights and molecular weight distributions were determined on a Shimadzu gel permeation chromatography (GPC) chromatograph containing a three-column bed (styragel HR 7.8 × 300 mm columns with 5 μm beads size; 100-5000, 500-30,000, and 2,000-4 × 10^6 Da), a Shimadzu RDI-10A differential refractometer, and a Shimadzu SPD-10A tunable absorbance

detector (254 nm). GPC samples were run in tetrahydrofuran at a flow rate of 1 ml/min at 35 ^{o}C and calibrated against polystyrene standards. Analysis was done using EZSTART 7.2 software. Gas chromatography analysis was performed on an Agilent 5890 Series II GC. The samples were heated from 40 ^{o}C to 100 ^{o}C at a ramp rate of 4 ^{o}C/min.

4.4.3 Synthesis of Homo- and Copolymers

In a typical experiment (entry 2, Table 3), in a N_2 filled glove box, a glass-lined Parr high-pressure reactor was charged with toluene (5 mL), AIBN (0.005 g), MA (0.3 g), and PPyH (0.1 g). The reactor was sealed, removed from glove box, and charged with ethene to 500 psi. The reaction mixture was allowed to stir in a 60 ^{o}C oil bath for 18 h. At the end of this period, the reactor was cooled, vented, and polymer was precipitated with a large excess of methanol. The polymer was collected by filtration and dried under high vacuum for 24 h. For those reactions, which did not require a Parr reactor, the polymerizations were carried out in 20 mL scintillation vials. The copolymer compositions were determined from ^{1}H-NMR integration of the methoxy protons versus the aliphatic resonances.

4.4.4 Kinetic Study of Methyl Acrylate Homopolymerization in the Presence of Different Acids

In a N_2-filled glovebox, MA (0.6 g), AIBN (0.005 g), acidic Al_2O_3 (0.071 g), toluene (5 mL) and tetrachloroethane (0.05 g) as internal standard were added into a reaction vessel equipped with a magnetic stirring bar. The reaction was stirred in 60 ^{o}C oil bath. GC samples were taken at different reaction times to determine MA conversion. With a constant acid to monomer molar ratio of 1/10, the same procedure was used for other Lewis and Brønsted acids.

4.4.5 Kinetic Study of Methyl Acrylate/ 1-Hexene Copolymerization in the Presence of Different Acids

In a N_2-filled glovebox, a reaction vessel equipped with a stirring bar was charged with MA (0.3 g), 1-hexene (1.0 g), AIBN (0.005g), acidic Al_2O_3 (0.036 g), toluene (5 mL) and tetrachloroethane (0.05 g).The reaction vessel was sealed and stirred in 60 ^{o}C oil bath. GC samples were taken at different reaction times to determine MA and hexene conversions. With a constant acid to monomer molar ratio of 1/10, the same procedure was used for other Lewis and Brønsted acids.

4.5 References

1. Boffa, L. S.; Novak, B. M. Chem Rev 2000, 100, 1479-1493.

2. Ittel, S. D.; Johnson, L. K.; Brookhart, M. Chem Rev 2000, 100, 1169-1204.

3. Liu, S.; Sen, A . J Polym Sci Part A: Polym Chem 2004, 42, 6175-6192.

4. Liu, S.; Elyashiv, S.; Sen, A. J Am Chem Soc 2001, 123, 12738-12739.

5. Elia, C.; Elyashiv, S.; Sen. A.; Lopez-Fernandez, R; Albeniz, A. C.; Espinet, P. Organometallics 2002, 21, 4249-4256.

6. Gu, B.; Liu, S.; Leber, D.; Sen, A. Macromolecules 2004, 37, 5142-5144.

7. Liu, S.; Gu, B.; Rowlands, H. A.; Sen, A. Macromolecules 2004, 37, 7924-7929.

8. Borkar, A.; Sen, A. Macromolecules 2005, 38, 3029-3032.

9. Nagel, M.; Poli, D.; Sen, A. Macromolecules 2005, 38, 7262-7265.

10. Tian, G. L.; Boone, H. W.; Novak, B. M. Macromolecules 2001, 34, 7656- 7663.

11. Venkatesh, R.; Klumperman, B. Macromolecules 2004, 37, 1226-1233.

12. Venkatesh, R.; Harrison, S.; Haddleton, D. M.; Klumperman, B. Macromolecules 2004, 37, 4406-4416.

13. Luo, R.; Sen, A. Macromolecules 2006, 39, 7798-7800.

14. Luo, R.; Sen, A. Macromolecules, 2007, 40, 154-156.

15. Lutz, J. F.; Kirci, B.; Matyjaszewski, K. Macromolecules 2003, 36, 3136-3145.

16. Isobe, Y.; Nakano, T.; Okamoto, Y. J Polym Sci Part A: Polym Chem 2001, 39, 1463-1471.

17. Lutz, J. F.; Jakubowski, W.; Matyjaszewski, K. Macromol Rapid Comm 2004, 25, 486-492.

18. Ray, B.; Isobe, Y.; Matsumoto, K.; Habaue, S.; Okamato, Y. Kamigaito, M.; Sawamoto, M. Macromolecules 2004, 37, 1702-1710.

19. Logothetis, A. L.; McKenna J. M. J Polym Sci Polym Chem Ed 1977, 15, 1431-1439.

20. Logothetis, A. L.; McKenna J. M. J. Polym Sci Polym Chem Ed 1978, 16, 2797-2802.

21. Eisenbach, C. D.; Sperlich, B. Macromolecules 1996, 29, 7748-7752.

Chapter 5

Electron Transfer Induced Iron-Based Atom Transfer Radical Polymerization of Styrene Derivatives and Copolymerization of Styrene and Methyl Methacrylate

5.1 Introduction

In the past decade, controlled radical polymerization (CRP) has emerged as a powerful technique for the synthesis of previously unattainable well-defined polymeric materials.[1] As one of the most important CRP techniques, atom transfer radical polymerization (ATRP) is based on the reversible reaction between a low oxidation state metal complex with an alkyl halide, which yields a high oxidation state metal complex and a radical.[2] This equilibrium results in a low radical concentration at any given time, thereby minimizing bimolecular termination reactions, and allowing the synthesis of polymers with predetermined molecular weight and narrow molecular weight distributions, as well as desired composition and architecture. [3-5]

Normal ATRP usually involves a combination of a relatively unstable lower oxidation-state metal complex (e.g., Cu(I) or Fe(II)) and an alkyl halide.[6] Reverse ATRP, using more stable metal species (Cu(II) or Fe(III)) and a radical source such as Azobis(isobutyronitrile) (AIBN), is generally more convenient.[7] However, reverse ATRP rarely allow the synthesis of pure block copolymers since the products are always contaminated with homopolymers formed by direct initiation from the free radical initiator.[8-9]

Recently, Matyjaszewski reported a new procedure for initiating ATRP whereby the active metal catalyst is generated by electron transfer (AGET) ATRP.[10-13] Specifically, active Cu(I) species is generated in situ from oxidatively stable Cu(II) via one-electron reduction by benign reducing agents such as tin 2-ethylhexanoate($Sn(EH)_2$) [12] or Vitamin C (ascorbic acid).[14]

In view of the known toxicity of copper compounds, we have sought to develop a more environmentally friendly AGET-ATRP system.

We report the first iron-based AGET-ATRP of styrene derivatives. Similar to copper-based AGET-ATRP, active Fe(II) species were generated by reducing air-stable Fe(III) bromide by FDA-approved $Sn(EH)_2$ or D-glucose (Scheme **5-1**). This redox reaction does not yield any other initiating radicals (Scheme **5-2**). Controlled polymerizations of styrene, 4-methylstyrene, 4-tert-butylstyrene, 4-acetoxystyrene and methyl 4-vinylbenzoate were successfully achieved by using 1-bromoethylbenzne as the initiator and $FeBr_3$/tributylamine/$Sn(EH)_2$ as the catalyst. Well-defined block copolymers were obtained by chain extension of polystyrene macroinitiators. Well-defined copolymers of styrene and methyl methacrylate (MMA) with adjustable content were also synthesized using this methodology.

Scheme **5-1:** Proposed mechanism for activator generated by electron transfer for atom transfer radical polymerization (AGET-ATRP)

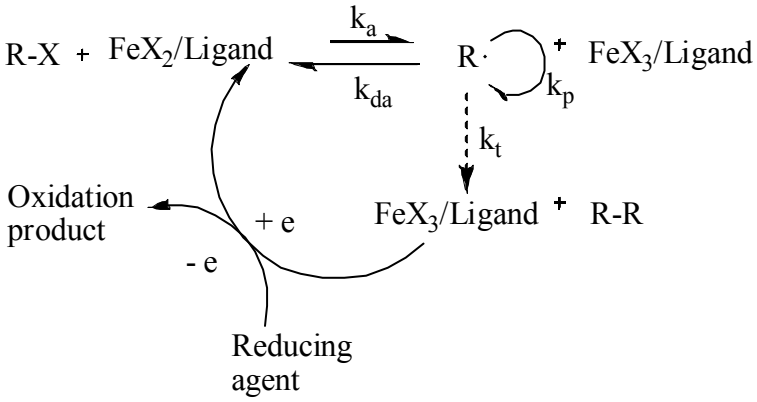

Scheme **5-2:** Reduction of Fe (III) to Fe (II) by Tin (II) 2-ethylhexanoate

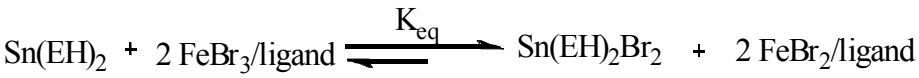

5.2 Results and Discussion

5.2.1 AGET-ATRP of Styrene Derivatives

A series of styrene derivatives were polymerized by the novel iron-based AGET-ATRP technique (Table **5-1**). The results show controlled polymerization for all the styrene derivatives examined. The apparent polymerization rate is the first order with respect to monomer concentration (Figure **5-1**), and molecular weight increases linearly with respect to total monomer conversion (Figure **5-2**). The obtained M_n values are in good agreement with theoretical numbers and the polydispersities are relatively low (less than 1.5, Figure **5-3**). As shown by entries 5 and 6, decreasing the amount of reducing agent resulted in decreased monomer conversion and a narrower PDI, which could be attributed to a higher concentration of deactivating Fe(III) species in the case of entry 6. As compared to normal Fe(II) catalyzed ATRP (entry 10, Table **5-1**), the iron-based AGET-ATRP showed a higher polymerization rate manifested by the higher monomer conversion for the same period of reaction time.

5.2.2 Styrene Polymerization in the Presence of Limited Amount of Air

As shown by entries 8 and 9 in Table **5-1**, the polymerizations remains well controlled even in the presence of a small amount of air. Presumably, the reducing agent maintains a steady concentration of the active Fe(II) species.

Table **5-1**: Electron transfer induced iron-catalyzed atom transfer radical polymerization(ATRP) of styrene derivatives[a]

Entry	Monomer	Monomer (g)	M/I[b]/$FeBr_3$/ $Sn(EH)_2$/L[b]	Conv (%)	$M_{n,exp}$[c] $\times 10^{-4}$	$M_{n,theo}$[d] $\times 10^{-4}$	PDI[c]
1	4-tButylstyrene	1.60	100/1/1/1/1	51	1.19	0.82	1.33
2	4-tButylstyrene	3.20	200/1/1/1/1	57	2.08	1.82	1.47
3	4-Methylstyrene	2.36	200/1/1/1/1	61	1.28	1.44	1.38
4	4-Methylstyrene	4.72	400/1/1/1/1	59	2.67	2.76	1.44
5	Styrene	2.08	200/1/1/1/1	61	1.92	1.26	1.35
6	Styrene	2.08	200/1/1/0.5/1	53	1.13	1.10	1.21
7	Styrene	4.16	400/1/1/1/1	68	2.67	2.83	1.20
8[e]	Styrene	2.08	200/1/1/1/1	65	1.67	1.35	1.27
9[e]	Styrene	4.16	400/1/1/1/1	57	2.23	2.37	1.13
10[f]	Styrene	2.08	200/1/1/1[f]	32	0.68	0.66	1.20
11	4-Acetoxystyrene	1.62	100/1/1/1/1	85	1.36	1.38	1.32
12	4-Acetoxystyrene	3.24	200/1/1/1/1	78	2.67	2.52	1.33
13	Methyl 4-vinylbenzoate	1.62	100/1/1/1/1	93	1.93	1.51	1.34
14	Methyl 4-vinylbenzoate	1.62	200/1/1/1/1	93	3.15	3.01	1.29

[a]Conditions: toluene, 1 mL; 110 ^oC, 2 h. [b] I, 1-bromoethylbenzene; L, tributylamine. [c]By GPC using polystyrene standards. [d]$M_{n,theo} = M_{monomer\ molar\ mass} \times ([M]_0/[I]) \times$ conversion. [e]Reactions in presence of limited amount of air. [f]Reaction using $FeBr_2$ as catalyst, M/I/$FeBr_2$/L=200/1/1/1.

5.2.3 Substitute Effects on Polymerization Rate: Hammett Plot

As shown by Figure **5-1**, monomers with electron-withdrawing substituents polymerize faster than those having electron-donating substituents. These results are in agreement with those from conventional radical polymerizations,[15] as well as previously reported controlled radical polymerizations.[16] Hammett plot (Figure **5-4**) give a linear relationship between the apparent rate constant and Hammett constants σ for different para-substituents. A ρ value of 1.59 was obtained for the iron-based AGET-ATRP, which is in good agreement with the ρ of 1.51 for copper-based ATRP reported by Matyjaszewski.[16] One possible explanation involves the effect of the substituent on the stability of the polystyryl halide. The partially positive carbon of the polarized C-X bond will be stabilized by electron donating substituents thereby lowering the ground-state energy of the dormant species.

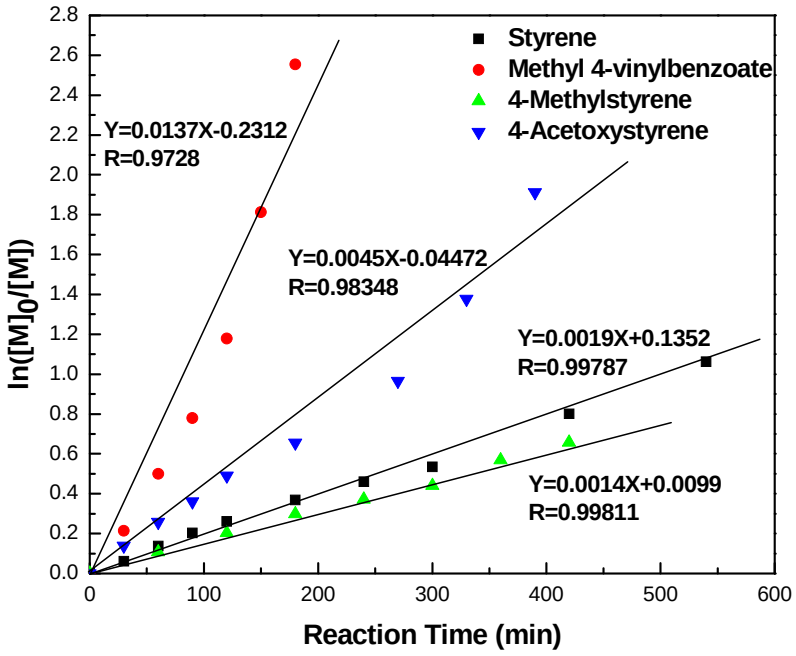

Figure **5-1**: Kinetics for electron transfer induced iron-catalyzed atom transfer radical polymerization (ATRP) of styrene derivatives. Conditions: Monomer, 0.02 mol; [M]/[1-Bromoethylbenzene]/[$FeBr_3$]/[$Sn(EH)_2$]/[Tributylamine] = 200/1/1/1/1; toluene, 5 mL; tetrachloroethane(TCE), 0.05 g as internal standard; 110 ^oC.

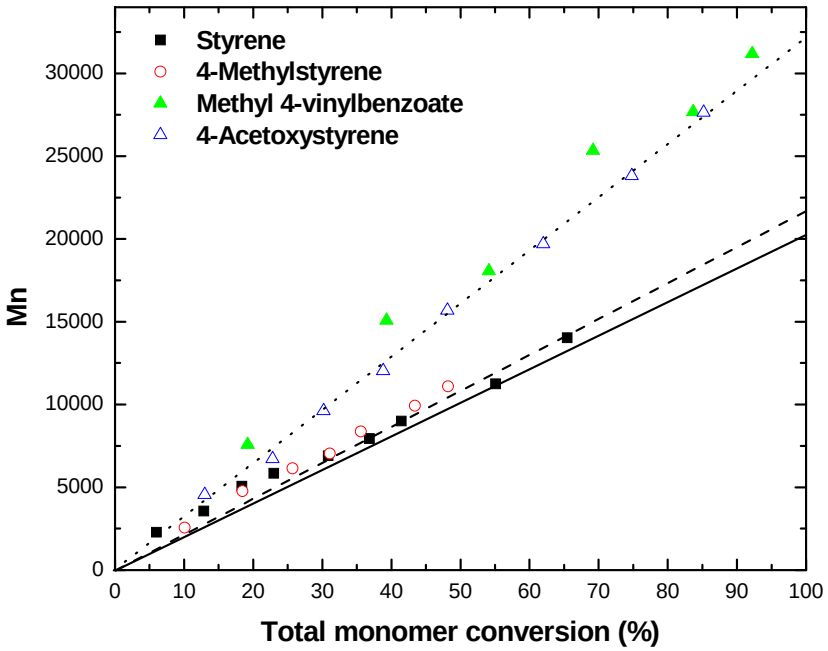

Figure **5-2**: Molecular weight dependence on total monomer conversion for electron transfer induced iron-catalyzed atom transfer radical polymerization (ATRP) of styrene derivatives. Conditions: Monomer, 0.02 mol; [M]/[1-Bromoethyl-benzene]/[$FeBr_3$]/[$Sn(EH)_2$]/ Tributylamine] = 200/1/1/1/1; toluene, 5 mL; tetrachloroethane (TCE), 0.05 g as internal standard; 110 ^oC.

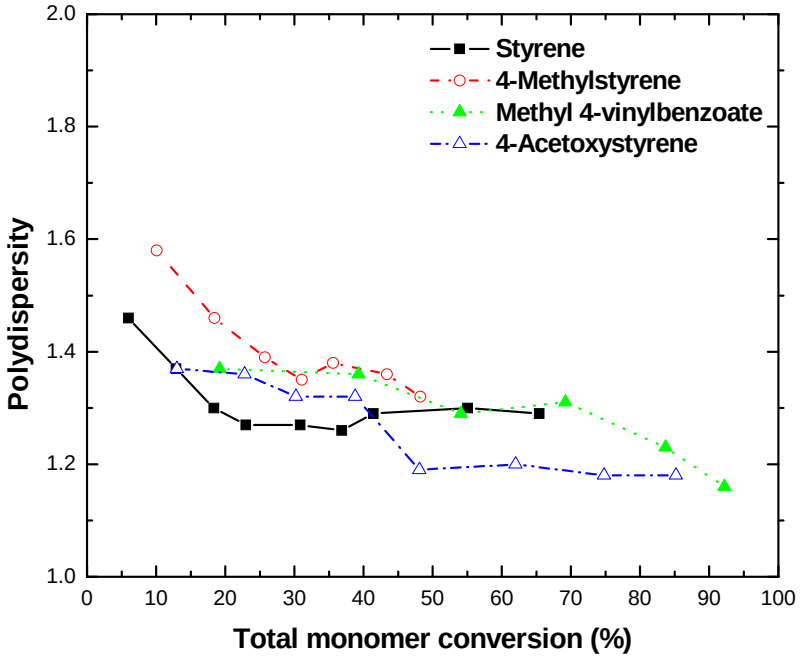

Figure **5-3**: Polydispersity vs. total monomer conversion for electron transfer induced iron-catalyzed atom transfer radical polymerization (ATRP) of styrene derivatives. Conditions: Monomer, 0.02 mol; [M]/[1-Bromoethylbenzene]/[$FeBr_3$]/[$Sn(EH)_2$]/ [Tributylamine] = 200/1/1/1/1; toluene, 5 mL; tetrachloroethane (TCE), 0.05 g as internal standard; 110 ^oC.

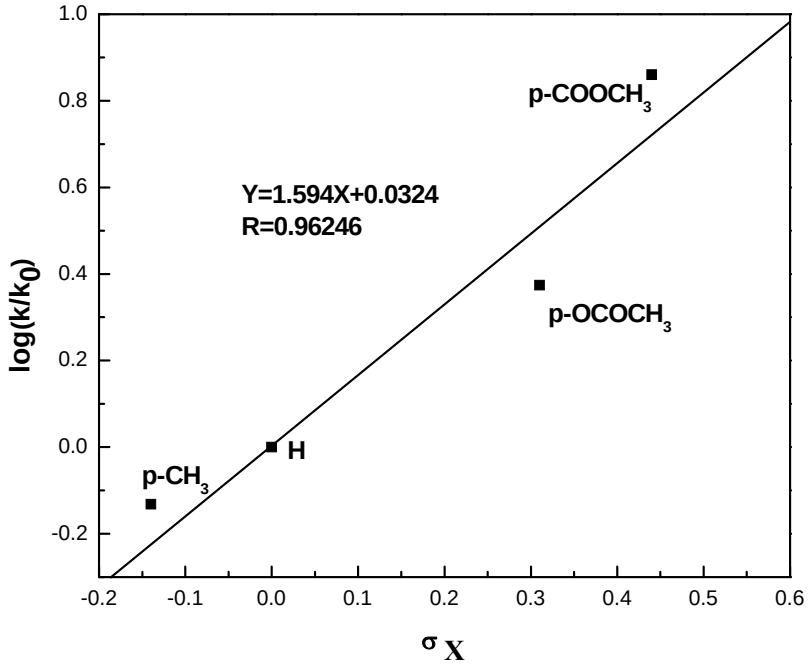

Figure **5-4**: Hammett plot for $k_{p(app)}$ in electron transfer induced iron catalyzed atom transfer radical polymerization (ATRP) of styrene derivatives. Conditions: Monomer, 0.02 mol; [M]/[1-Bromoethylbenzene]/[$FeBr_3$]/[$Sn(EH)_2$]/ [Tributylamine] = 200/1/1/1/1; toluene, 5 mL; tetrachloroethane (TCE), 0.05 g as internal standard; 110 ^oC.

5.2.4 Effects of Varying Iron Concentration

Table **5-2** summarizes a series of experiments in which styrene was polymerized in presence of different concentration of the iron-based catalyst. The amount of iron varied from 0.1 mmol to as low as 0.01 mmol. According to Table 2, the polymerization rate decreased with the reduction in the concentration of iron species. With 0.1 mmol iron (Entry 1), 80.2% conversion was obtained after 3 h reaction, while with 0.01 mmol iron (Entry 3), only 44.2% conversion was obtained. However, the system remained well-controlled at all iron concentrations. Figure **5-5** shows the first-order polymerization kinetics and Figure **5-6** shows good control over the molecular weight and polydispersity using only 0.01 mmol iron catalyst.

Decreasing the amount of iron catalyst has the advantage of decreasing the metal residue in the final product, e.g. the product from entry 1 is an orange powder while the products from entries 3 and 4 are white.

5.2.5 Styrene Polymerization in the Presence of Glucose as Reducing agent

AGET-ATRP of styrene was also carried out in the presence of D-glucose as the reducing agent (Table 3). Although the monomer conversion for the same time period was lower than that in the presence of $Sn(EH)_2$, a stronger reducing agent, the system is well controlled.

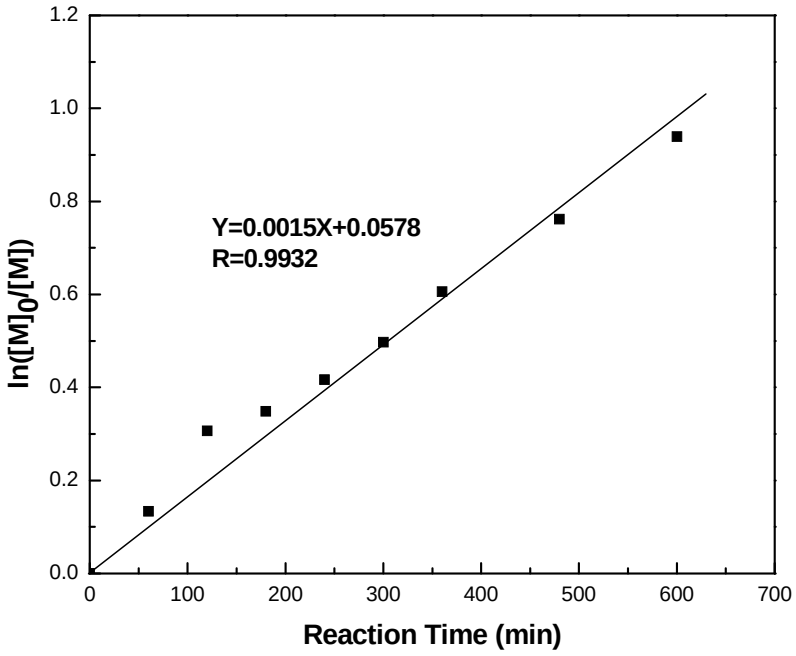

Figure **5-5**: Kinetics for electron transfer induced atom transfer radical polymerization (ATRP) of styrene at low iron concentration. Conditions: Monomer, 0.02 mol; [M]/[1-Bromoethylbenzene]/[$FeBr_3$]/[$Sn(EH)_2$]/[Tributylamine] = 200/1/0.1/0.1/0.1; toluene, 5 mL; tetrachloroethane (TCE), 0.05 g as internal standard; 110 ^oC.

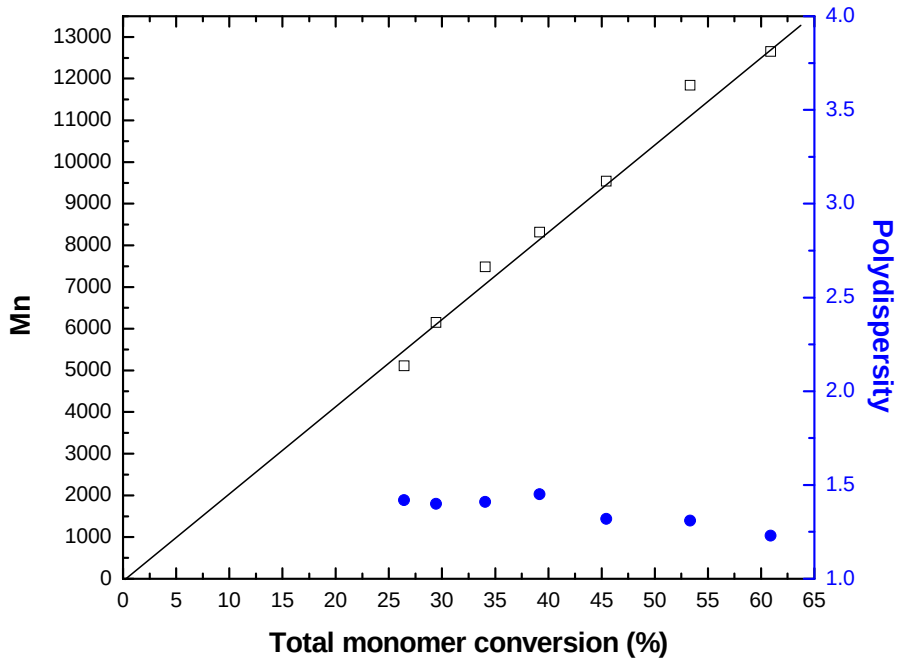

Figure **5-6**: Molecular weight and polydispersity dependence on total monomer conversion for electron transfer induced atom transfer radical polymerization (ATRP) of styrene at low iron concentration. Conditions: Monomer, 0.02 mol; [M]/[1-Bromoethylbenzene]/ [$FeBr_3$]/[$Sn(EH)_2$]/[Tributylamine] = 200/1/0.1/0.1/0.1; toluene, 5 mL; tetrachloroethane (TCE), 0.05 g as internal standard; 110 ^oC.

Table **5-2**: Effect of iron concentration on electron transfer induced atom transfer radical polymerization (ATRP) of styrene[a]

Entry	Molar ratio St/I[b]/ $FeBr_3$/ $Sn(EH)_2$/ L[b]	Iron (mmol)	Time (h)	Conv. (%)	$M_{n,theo}$[c] $\times 10^4$	$M_{n,expt}$[d] $\times 10^4$	PDI[d]
1	200/ 1/ 1/ 1/ 1	0.1	3	80.2	1.67	1.52	1.18
2	200/ 1/ 0.5/ 0.5/ 0.5	0.05	3	77.9	1.62	1.53	1.26
3	200/ 1/ 0.1/ 0.1/ 0.1	0.01	3	44.2	0.92	1.05	1.28
4	200/ 1/ 0.1/ 0.1/ 0.1	0.01	17	87.4	1.82	2.03	1.23

[a]Conditions: Styrene, 2.08 g (0.02 mol); toluene, 1 mL; 110 °C. [b]I, 1-bromoethylbenzene; L, tributylamine [c]$M_{n,theo} = M_{monomer\ molar\ mass} \times ([M]_0/[I]) \times$ conversion. [d]By GPC using polystyrene standards.

Table **5-3**: Electron transfer induced iron-catalyzed atom transfer radical polymerization (ATRP) of styrene in the presence of D-glucose as reducing agent[a]

Entry	Styrene (g)	M/I[b]/$FeBr_3$/glucose/L[b]	Conv. (%)	$M_{n,exp}$[c] $\times 10^{-4}$	$M_{n,theo}$[d] $\times 10^{-4}$	PDI[c]
1	2.08	200/1/1/1/1	24	0.56	0.50	1.19
2	4.16	400/1/1/1/1	29	1.04	1.21	1.23

[a]Conditions: toluene, 1 mL; 110 °C, 2 h. [b]I, 1-bromoethylbenzene; L, tributylamine. [c]By GPC using polystyrene standards. [d]$M_{n,theo} = M_{monomer\ molar\ mass} \times ([M]_0/[I]) \times$ conversion.

5.2.6 Extension of Polystyrene Macroinitiator by AGET-ATRP

The "living" nature of this iron-based AGET-ATRP system was further confirmed by treating the macroinitiator made by this technique with a different monomer for chain extension using similar conditions. For example, an bromo-functionalized polystyrene macroinitiator (M_n = 714, PDI = 1.32) (71 mg, 0.1 mmol) prepared by AGET-ATRP was employed to polymerize 4-methyl styrene (2.36 g) using 0.1 mmol Fe catalyst at 110^{o}C. The GPC analysis of the resulted block copolymer revealed the expected increased molecular weight (M_n, 13031; PDI, 1.25) and no detectable amount of unreacted starting block (Figure **5-7** (a)). Similarly, a block copolymer of styrene and 4-tert-butylstyrene was synthesized through this method (Figure **5-7** (b)).

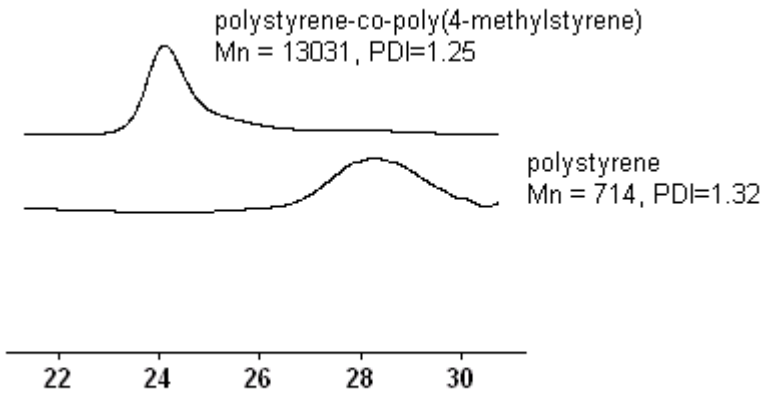

(a)

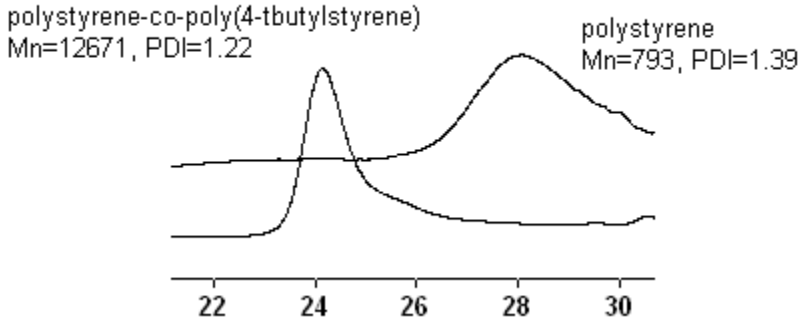

(b)

Figure **5-7**: Chain extension of polystyrene macroinitiator prepared by electron transfer induced iron-catalyzed atom transfer radical polymerization (ATRP) with (a) poly(4-methyl styrene) and (b) poly(4-tertbutylstyrene).

5.2.7 Copolymerization of Styrene and Methyl Methacrylate

Copolymerization of styrene and methyl methacrylate was carried out with the same methodology using either $Sn(EH)_2$ and D-glucose as the reducing agent (Table **5-4**). The copolymer compositions were determined by ^1H NMR integration of the aliphatic proton vs. the aromatic protons (Figure **5-8**). The gel permeation chromatography showed only one peak with both refractive index (RI) and UV detector, which indicates a true copolymer over the entire molecular weight distribution range. The homopolymerization of MMA was not controlled with polydispersity of 1.98, as were the copolymerizations with high MMA/styrene feed ratios. However, higher amounts of styrene in the feed led to well controlled polymerizations with low polydispersities, suggesting higher selectivity of the iron-based catalyst for the polystyryl radical. As with styrene homopolymerization, the use of the weaker reducing agent, D-glucose, resulted in lower yields but the polymerizations remained well-controlled.

Table **5-4**: Copolymerization of styrene and methyl methacrylate using electron transfer induced iron-catalyzed atom transfer radical polymerization (ATRP).[a]

Entry	MMA (g)	[Styrene]/[MMA] (mol ratio)	Yield (%)	MMA Incorp. (%)	$M_{n,exp}$[b] $\times 10^{-4}$	$M_{n,theo}$[c] $\times 10^{-4}$	PDI[b]
1[d]	2.00	0	54.5	100	1.73	2.18	1.98
2[d]	1.33	1:2	55.8	63.7	2.60	2.26	1.48
3[d]	1.00	1:1	50.4	47.6	2.42	2.06	1.38
4[d]	0.67	2:1	53.4	37.3	2.33	2.19	1.20
5[e]	1.00	1:1	11.7	54.9	0.30	0.48	1.28
6[e]	0.67	2:1	22.2	29.5	0.67	0.74	1.21

[a]Conditions: [M]/[1-bromoethylbenzene]/[$FeBr_3$]/[L]/[Reducing agent] = 400/1/1/1/1, toluene, 1 mL; 110 ^oC, 2 h. [b]By GPC using polystyrene standards. [c]$M_{n,theo} = M_{monomer\ molar\ mass} \times ([M]_0/[I]) \times$ conversion. [d]Coplymerizations using $Sn(EH)_2$ as reducing agent. [e]Copolymerizations using D-glucose as reducing agent.

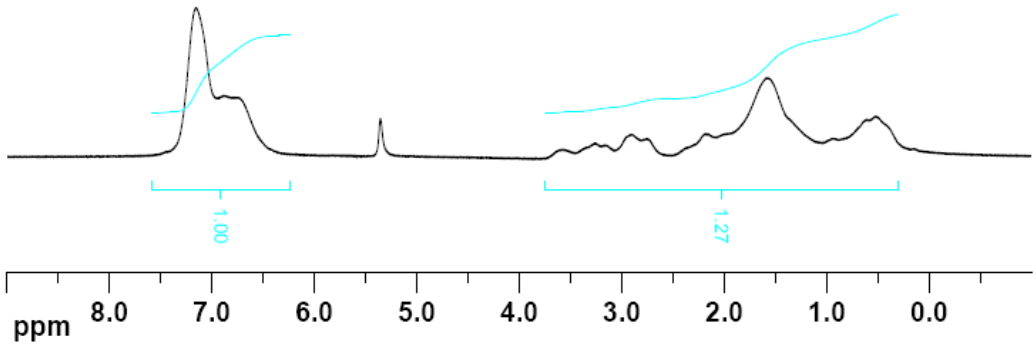

Figure **5-8**: ^{1}H NMR spectrum of styrene and methyl methacrylate(MMA) with 29 mol% MMA incorporation.

5.3 Conclusion

The first oxidatively stable and environmentally friendly iron-based AGET-ATRP system for styrene derivatives has been reported. Similar to previously reported copper-based system, the reducing agents $Sn(EH)_2$ and D-glucose were employed to generate the active Fe(II) species in situ. Monomers with electron-withdrawing substituents polymerize faster than those having electron-donating substituents. The amount of iron catalyst could be reduced to as a low as 0.01 mmol while retaining sufficient activity to impart control. Well-defined copolymers of styrene and MMA were also synthesized through this method.

5.4 Experimental Procedure

5.4.1 Materials

All chemicals and reagents were obtained from Aldrich unless otherwise stated. Styrene (99%), 4-methylstyrene (96%), 4-tert-butylstyrene (93%) 4-acetoxystyrene (96%) and methyl methacrylate (99%) were passed through basic alumina and dried over calcium hydride before use. Methyl 4-vinylbenzoate (97%), 1-bromoethylbenzene (97%), iron(III) bromide (98%), tin(II) 2-ethylhexanoate ($Sn(EH)_2$) (95%), tributylamine (98.5%) and D-glucose (99%) were used as received.

5.4.2 Instrumentation

^{1}H- and ^{13}C-NMR spectra were recorded using a Bruker 300-DPX spectrometer at ambient temperature (^{1}H-NMR, 300 MHz; ^{13}C-NMR, 75 MHz). Chemical shifts are referenced to $CDCl_3$. Molecular weights and polydispersities were determined on a Shimadzu gel permeation chromatography (GPC) chromatograph containing a three-column bed (styragel HR 7.8 × 300 mm columns with 5 μm beads size; 100-5000, 500-30,000, and 2,000-4 × 10^6 Da), a Shimadzu RDI-10A differential refractometer, and a Shimadzu SPD-10A tunable absorbance detector (254 nm). GPC samples were run in tetrahydrofuran at a flow rate of 1 ml/min at 35^{o}C and calibrated against polystyrene standards. Analysis was done using EZSTART 7.2 software. Gas chromatography(GC) analysis was performed on an Agilent 5890 Series II GC. The samples were heated from 40 ^{o}C to 100 ^{o}C at a ramp rate of 4 ^{o}C/min.

5.4.3 Kinetics of AGET-ATRP of Styrene Derivatives

In a N_2-filled dry box, a round bottom flask equipped with a magnetic stir bar was charged with degassed styrene (2.08 g, 0.02 mol), $FeBr_3$ (29.5 mg, 0.1 mmol), $Sn(EH)_2$ (40.5 mg, 0.1 mmol), tributylamine (18.5 mg, 0.1 mmol), internal standard tetrachloroethane (TCE, 0.05 g), and toluene (5 mL). The mixture was stirred for 10 min before 1-bromoethylbenzene (18.5 mg, 0.1 mmol) was added to initiate the polymerization. After the initial sample was taken, the flask was sealed and placed in an oil bath at 110^{o}C. Samples were taken at specific time intervals using a syringe and analyzed by GC. The conversion of styrene was calculated from the integration of styrene peak with respect to TCE peak. The molecular weight was measured by GPC.

5.4.4 General Procedure for AGET-ATRP of Styrene Derivatives

In a N_2-filled dry box, a round bottom flask equipped with a magnetic stir bar was charged with degassed styrene (2.08 g, 0.02 mol), $FeBr_3$ (29.5 mg, 0.1 mmol), $Sn(EH)_2$ (40.5 mg, 0.1 mmol), tributylamine (18.5 mg, 0.1 mmol), and toluene (1 mL). The mixture was stirred for 10 min before 1-bromoethylbenzene (18.5 mg, 0.1 mmol) was added to initiate the polymerization. The flask was sealed and placed in an oil bath at 110^{o}C for 2 h. At the end of this period, the polymer was precipitated with a large excess of hexane and washed with methanol. The polymer (Yield = 1.27 g, $M_n = 1.26\times10^4$ g/mol, PDI = 1.35) was collected by filtration and dried under high vacuum for 24 h.

5.4.5 General Procedure for Block Copolymer Formation: Preparation of Poly(4-Methylstyrene)-*b*-Polystyrene

In a N_2-filled dry box, a polystyrene macroinitiator (M_n = 714, PDI = 1.32) (71 mg, 0.1 mmol) prepared by AGET-ATRP, was dissolved in 4-methylstyrene (2.36 g, 0.02 mol) in a round bottom flask. The flask was then charged with $FeBr_3$ (29.5 mg, 0.1 mmol), $Sn(EH)_2$ (40.5 mg, 0.1 mmol), tributylamine (18.5 mg, 0.1 mmol), and toluene (1 mL). The mixture was stirred for 10 min before 1-bromoethylbenzene (18.5 mg, 0.1 mmol) was added to initiate the polymerization. The flask was sealed and placed in an oil bath at 110^{o}C for 4 h. At the end of this period, the polymer was precipitated with a large excess of hexane and washed with methanol. The polymer (M_n = 13031, PDI = 1.25) was collected by filtration and dried under high vacuum for 24 h.

5.4.6 General Procedure for AGET-ATRP of Styrene in the Presence of Limited Amount of Air

In a N_2-filled dry box, a round bottom flask equipped with a magnetic stir bar was charged with degassed styrene (2.08 g, 0.02 mol), $FeBr_3$ (29.5 mg, 0.1 mmol), $Sn(EH)_2$ (40.5 mg, 0.1 mmol), tributylamine (18.5 mg, 0.1 mmol), and toluene (1 mL). The mixture was stirred for 10 min before 1-bromoethylbenzene (18.5 mg, 0.1 mmol) was added to initiate the polymerization. The contents of the flask were exposed to air for 5 min and then sealed and placed in an oil bath at 110^{o}C for 2 h. At the end of this period, the polymer was precipitated with a large excess of hexane and washed with methanol. The polymer (Yield = 1.35 g, $M_n = 1.35\times10^4$ g/mol, PDI = 1.27) was collected by filtration and dried under high vacuum for 24 h.

5.4.7 General Procedure for AGET-ATRP of Styrene in the Presence of Glucose as Reducing Agent

In a N_2-filled dry box, a round bottom flask equipped with a magnetic stir bar was charged with degassed styrene (2.08 g, 0.02 mol), $FeBr_3$ (29.5 mg, 0.1 mmol), D-glucose (18.0 mg, 0.1 mmol), tributylamine (18.5 mg, 0.1 mmol), and toluene (1 ml). The mixture was stirred for 10 min before 1-bromoethylbenzene (18.5 mg, 0.1 mmol) was added to initiate the polymerization. The flask was sealed and placed in an oil bath at 110^{o}C for 2 h. At the end of this period, the polymer was precipitated with a large excess of hexane and washed with methanol. The polymer (Yield = 0.50g, $M_n = 0.5\times10^4$ g/mol, PDI = 1.19) was collected by filtration and dried under high vacuum for 24 h.

5.4.8 General Procedure for AGET-ATRP Copolymerization of Styrene and Methyl Methacrylate

In a N_2-filled dry box, a round bottom flask equipped with a magnetic stir bar was charged with degassed styrene (1.04 g, 0.01 mol), methyl methacrylate (1.00 g, 0.01 mol), $FeBr_3$ (14.8 mg, 0.05 mmol), $Sn(EH)_2$ (20.3 mg, 0.05 mmol), tributylamine (9.3 mg, 0.05 mmol), and toluene (1 mL). The mixture was stirred for 10 min before 1-bromoethylbenzene (9.3 mg, 0.05 mmol) was added to initiate the polymerization. The flask was sealed and placed in an oil bath at 110^{o}C for 2 h. At the end of this period, the polymer was precipitated with a large excess of hexane and washed with methanol. The polymer (Yield = 1.03 g, $M_n = 2.42\times10^4$ g/mol, PDI = 1.38) was collected by filtration and dried under high vacuum for 24 h.

5.5 References

1. *Advances in Controlled/Living Radical Polymerization*; Matyjaszewski, K., Ed.; American Chemical Society: Washington, DC, 2003; Vol. 854.
2. Matyjaszewski, K.; Xia, J. *Chem. Rev.* **2001**, *101*, 3689-3745.
3. Coessens, V.; Pintauer, T.; Matyjaszewski, K. *Prog. Polym. Sci.* **2001**, *26*, 337-377.
4. Davis, K. A.; Matyjaszewski, K. *Adv. Polym. Sci.* **2002**, *159*, 1-166.
5. Gao, H.; Tsarevsky, N.V.; Matyjaszewski, K. *Macromolecules* **2005**, *38*, 5995-6004.
6. Zhu, S.; Yan, D. *Macromolecules* **2000**, *34*, 8233-8238.
7. Zhu, S.; Yan, D.; Zhang, G. *J. Polym. Sci., A: Polym. Chem.* **2001**, *39*, 765-774.
8. Gromada, J.; Matyjaszewski, K. *Macromolecules* **2001**, *34*, 7664-7671.
9. Li, M.; Jahed, N. M.; Min, K.; Matyjaszewski, K. *Macromolecules* **2004**, *37*, 2434-2441.
10. Min, K.; Gao, H.; Matyjaszewski, K. *J. Am. Chem. Soc.* **2005**, *127*, 3825-3830.
11. Jakubowski, W.; Matyjaszewski, K. *Macromolecules* **2005**, *38*, 4139-4146.
12. Jakubowski, W.; Min, K.; Matyjaszewski, K. *Macromolecules* **2006**, *39*, 39-45.
13. Jakubowski, W.; Matyjaszewski, K. *Angew. Chem.* **2006**, *118*, 4594-4598.
14. Min, K.; Gao, H.; Matyjaszewski, K. *Macromolecules* **2007**, *40*, 1789-1791.
15. Imoto, M.; Kinoshita, M.; Nishigaki, M. *Makromol. Chem.* **1965**, *86*, 217.
16. Qiu, J.; Matyjaszewski, K. *Macromolecules* **1997**, *30*, 5643-5648.

Chapter 6

Palladium-Catalyzed Non-alternating Copolymerization of Ethene and Carbon Monoxide: Scope and Mechanism

6.1 Introduction

The palladium-catalyzed alternating copolymerization of ethene and carbon monoxide (CO) has been studied extensively over the last two decades.[1,2] The resultant polyketone is difficult to process because of its insolubility in common solvents and its high melting point (~265 °C) brought about by the interchain dipolar interaction between carbonyl groups present at 50% level in the copolymer. The problem of processibility can be circumvented by lowering the carbon monoxide content in the copolymer. It has been suggested that as low as ~5–10 mol% carbon monoxide incorporation into polyethene would be sufficient to impart such desirable properties as adhesion, paintability and hardness without sacrificing the processibility associated with polyethene.[1,2] However, such material is not attainable using the conventional catalysts, which produce strictly alternating ethene/carbon monoxide copolymers even at high ethene/carbon monoxide ratios. While these catalysts are capable of oligomerizing ethene[3], consecutive ethene insertions are not observed in the presence of carbon monoxide due to the formation of a stable five-membered chelate following sequential ethene/CO insertion, which can only be opened by the strongly coordinating carbon monoxide but not by ethene (Scheme1).[4–7,11] Double carbon monoxide insertions do not occur due to thermodynamic reasons.[8–9]

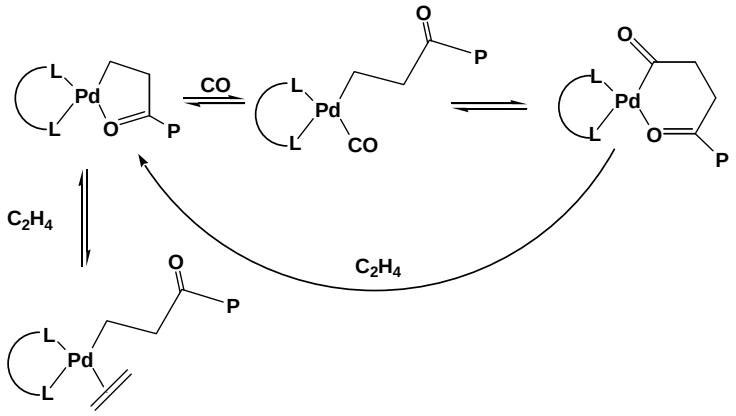

Scheme **6-1**: General catalytic cycle for ethene/carbon monoxide co-polymerization.

Recently, first Drent[10] and then we[11] and others[12] have reported on palladium complexes with anionic phosphine-sulfonate ligand ($P\sim SO_3^-$) that are able to form non-alternating ethene/CO copolymers, where multiple ethene insertions were believed to be enabled by electronic destabilization of the five-membered chelate.[10]

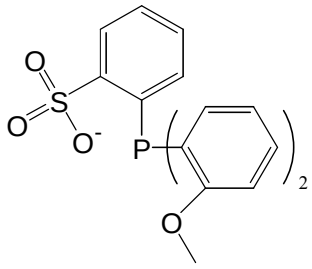

$P\sim SO_3^-$ Ligand

Herein, we report on the copolymerization of ethene with carbon monoxide with very low carbon monoxide content. Further, we have examined in detail the mechanism of the non-alternating copolymerization through a combination of monomer binding thermodynamics and monomer insertion kinetics. The results obtained are significantly different from that observed with traditional alternating copolymerization catalysts[5,13] and provide a more detailed explanation for the observed non-alternation in the phosphine-sulfonate coordinated palladium system.

6.2 Results and Discussion

6.2.1 Polymerizations using catalyst formed in situ

The in situ combination of the anionic phosphine-sulfonate ligand and Palladium acetate ($Pd(OAc)_2$) formed an active catalyst for the copolymerization of ethene and carbon monoxide. Results of the copolymerization of ethene and carbon monoxide are summarized in Table **6-1**. As shown, the copolymer composition can be tuned by varying the ethene/carbon monoxide feed ratio. Entries 2, 3, and 6 were conducted under the same reaction conditions but with different carbon monoxide loadings. By increasing the carbon monoxide loading from 15 to 25 psi, the carbon monoxide content in the final product increased from 6 to 32 mol%. However, as noted previously[11], the copolymer yield decreased with increased carbon monoxide content. As shown by entries 3, 4 and 5, under the same reaction conditions, the carbon monoxide content in the copolymer decreased with increasing reaction temperature, which was predicted by Ziegler's computational results.[14]

The non-alternating copolymer structure was confirmed by ^{1}H NMR (Figure **6-1**) and ^{13}C NMR spectroscopy (Figure **6-2**). For the ^{1}H NMR spectrum, the resonance at 2.7 ppm was assigned to CH_2 in alternating copolymer segments. The resonances at 2.4 ppm and 1.6 ppm were assigned to the CH_2 α and β to the carbonyl, respectively for consecutive ethene insertions. The resonance at 1.3 ppm was assigned to ethene units not adjacent to a carbonyl. For ^{13}C NMR spectrum, multiple peaks near 210 ppm indicated different chemical environments for the carbonyl groups in the final product. Double, triple and quadruple ethene insertions were also indicated by signals between 20 ppm and 45 ppm (Figure **6-2**). The chemical shift assignments are in good agreement with previously reported values for non-alternating polyketones.[10]

Table **6-1**: Results of the in situ copolymerization of CO and C_2H_4 [a]

Entry	Temp. (°C)	CO (psi)	Yield (g)	Activity (g $mmol^{-1}h^{-1}$)	CO Incorp. mol%[b]	Melting Point (°C)	M_n (PDI)[c]
1	90	0	0.657	4.38	0	125.4	-
2	90	15	0.423	2.82	6	120.8	-
3	90	20	0.327	2.18	10	117.9	4460 (3.5)
4	80	20	0.172	1.15	28	115.9	-
5	110	20	0.696	4.64	8	120.2	-
6	90	25	0.206	1.37	32	97.2	37555 (2.1)
7	110	25	0.740	4.94	9	118.8	-

[a]Reaction conditions: Ethene, 300 psi; $Pd(OAc)_2$, 0.1 mmol; (P~SO3H), 0.1 mmol; CH2Cl2, 10 mL; 1.5 h. [b]By 1H NMR spectroscopy. [c]By high temperature GPC using polystyrene standards.

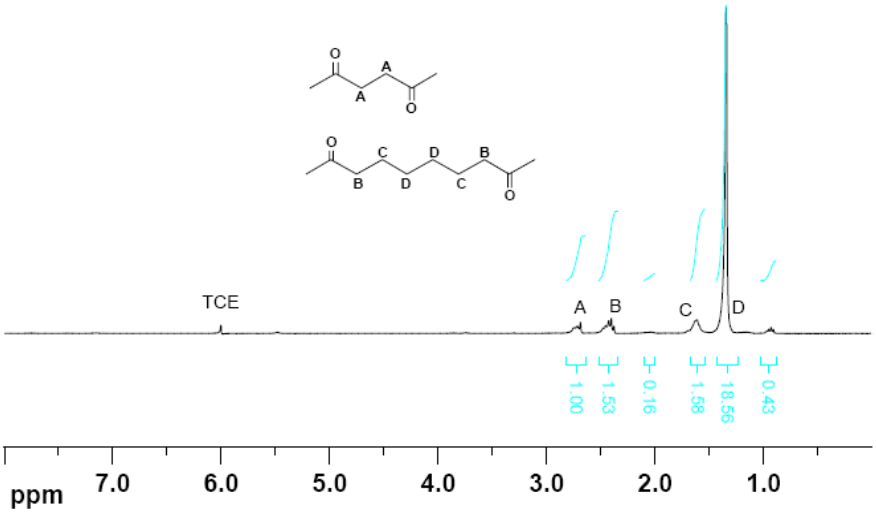

Figure **6-1**: ^{1}H NMR spectrum (in tetrachloroethane-d_2, TCE) of non-alternating polyketone with 10 mol% CO incorporation.

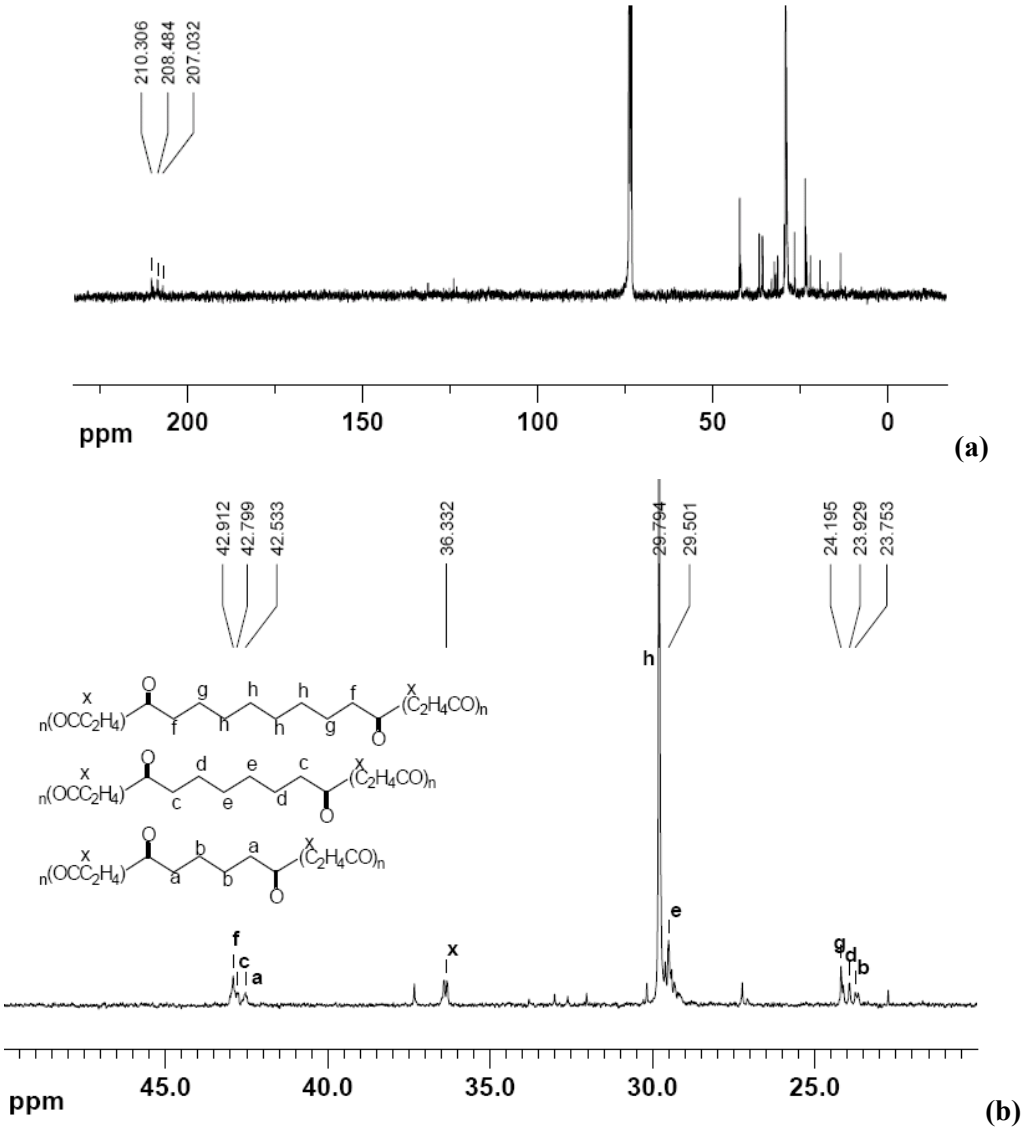

Figure **6-2**: ^{13}C NMR spectrum (in tetrachloroethane-d_2, TCE) of non-alternating polyketone with 10 mol% CO incorporation. (a) ^{13}C NMR spectrum, and (b) expansion of the methylene region of ^{13}C NMR spectrum.

6.2.2 DSC of the non-alternating polyketone

A single melting point was found for all the materials synthesized, confirming the formation true copolymers of ethene and carbon monoxide (Figure **6-3**). In copolymers with low CO content, the melting point decreases with increasing carbon monoxide content, presumably due to the disruption of polyethene crystallinity. For example, increasing CO content from 1 mol% to 10 mol% decreased the melting point from 125.3 °C to 117.9 °C.

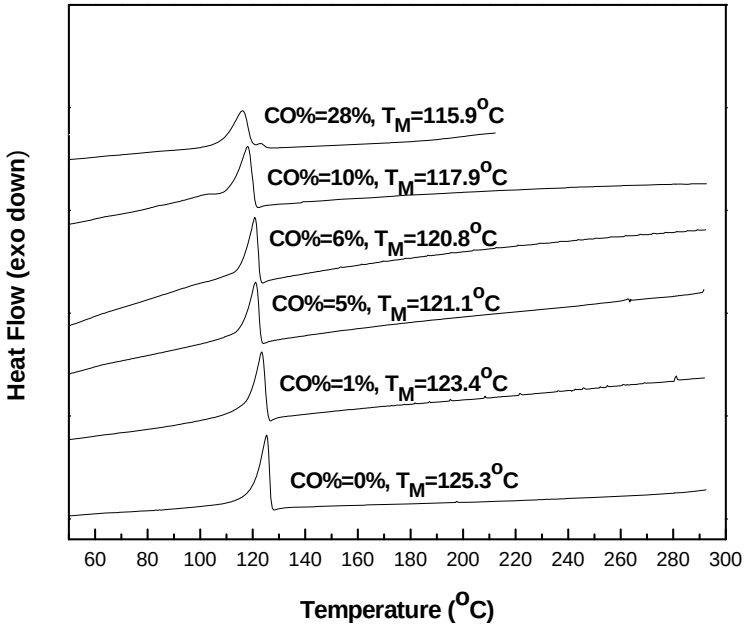

Figure **6-3**: Melting point of nonalternating polyketone by differential scanning calorimetry.

6.2.3 IR spectra of the non-alternating polyketone

The abnormally low $\nu_{C=O}$ (~1695 cm^{-1}) of the carbonyl groups in the alternating ethene/carbon monoxide copolymer in the solid state has been noted previously.[15] This phenomenon is due to the presence of intra- and interchain dipolar interactions between the carbonyl groups. The IR spectra of nonalternating polyketones are consistent with this hypothesis. As shown in Figure **6-4**, the carbonyl peak shifts from 1717 cm^{-1} (1 mol% CO) to 1689 cm^{-1} (49 mol% CO) with increasing carbon monoxide content in the copolymer.

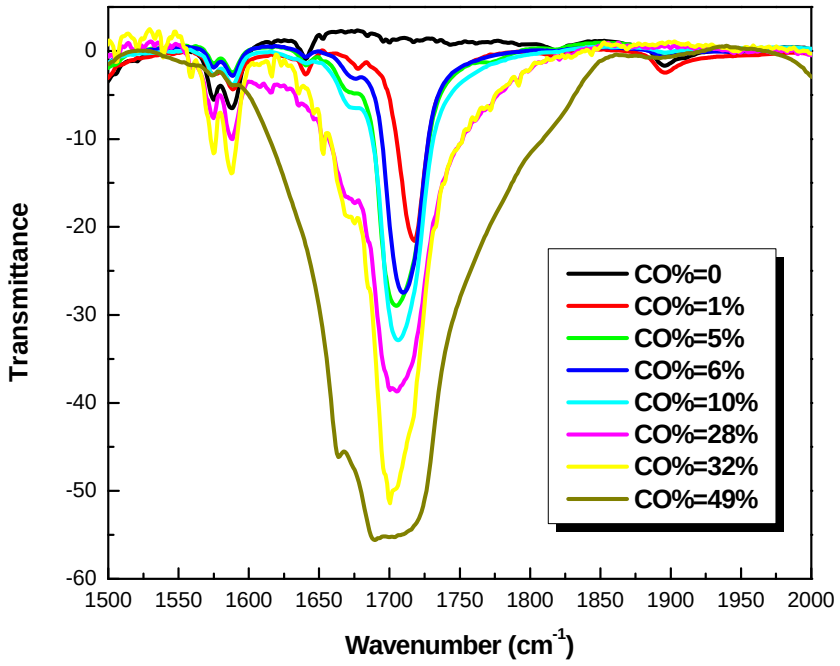

Figure **6-4**: Carbonyl region of the IR spectra (KBr) of non-alternating polyketones with differing CO content.

6.2.4 Mechanistic study of non-alternating ethene/CO copolymerization.

In order to examine the unique properties of the phosphine-sulfonate catalyst that give rise to non-alternation, we constructed a complete catalytic cycle for the non-alternating copolymerization of CO and ethene.

Preparation of (P~SO_3)Pd(CH_3)(Py) 1

We used a well-defined model compound with a methyl group and pyridine occupying the two coordination sites for the following kinetics study. This complex was characterized by ^{1}H- and ^{31}P NMR spectroscopy and single-crystal X-ray diffraction. The crystal structure was reported previously by our group.[11]

Synthesis of five-membered chelate (P~SO_3)Pd($CH_2CH_2C(O)CH_3$) 3 by step-wise insertion

To accomplish this, **1** was treated with 50 psi CO, causing immediate formation of (P~SO_3)Pd($C(O)CH_3$)(Py) **2**. The ^{1}H NMR signal for Pd–CH_3 at 0.2 ppm was replaced by Pd–$COCH_3$ at 1.8 ppm. The ^{31}P NMR signal at 22.7 ppm was replaced by a signal at 10.8 ppm, and a ^{13}C NMR signal appeared at 227 ppm. IR analysis showed carbonyl absorption at 1695 cm^{-1}, and single-crystal X-ray diffraction also confirmed the formation of **2**.[11]

When a solution of **2** in CD_2Cl_2 was exposed to 80 psi ethene at 50^{o}C for 5 min, slow insertion of ethene into the Pd-acyl bond occurred to give a mixture of **3** and unreacted **2**. ^{1}H NMR analysis showed a new terminal methyl group at 1.9 ppm, and the CH_2 groups α and β to the metal center appeared as a doublet of triplet at1.3 ppm and as a broad multiplet at 2.1 ppm

respectively. Also a new ^{31}P NMR signal appeared at 23.6 ppm and a broad ^{13}C NMR carbonyl signal appeared at 216 ppm. IR analysis showed carbonyl absorption at 1643 cm^{-1}, which is consistent with the formation of a five membered chelate like **3**.

Determination of the equilibrium constant between (P~SO_3)Pd($CH_2CH_2C(O)CH_3$) 3 and (P~SO_3)Pd($CH_2CH_2C(O)CH_3$)(C_2H_4) 4

The five-membered chelate **3** was generated in situ using the above method. Subsequent exposure of **3** to ethene confirmed generation of an equilibrium mixture of **3** and **4**. The NMR data of **4** was listed in the experimental section. The temperature dependent equilibrium was studied in CD_2Cl_2 from −90 to −70 °C. The Van't Hoff plot (Figure **6-5**) gives ΔH^o= 0.68 ± 0.07 kcal/mol and ΔS^o= −1.1 ± 0.3 eu. The calculated equilibrium constant K_1 at 25 ^oC is 0.548 M^{-1}.

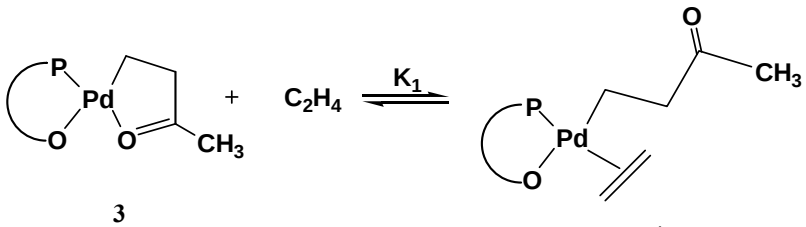

3 **4**

Since impure starting material **3** was used, the impurity **2** could influence the reaction by binding with ethene. This would result in an over estimation of K_1 because the insertion and binding of ethene to **2** contributes to the concentration of **4**.

Table **6-2**: Equilibrium constants for **3** + C_2H_4 ⇌ **4** from −90 °C to −70 °C

Temperature (K)	K_1 (M^{-1})	[**4**] : [**3**]	[Ethene] (*M*)
183	0.265	0.0897	0.339
188	0.288	0.0852	0.296
193	0.297	0.0825	0.278
198	0.309	0.0815	0.263
203	0.321	0.0803	0.250

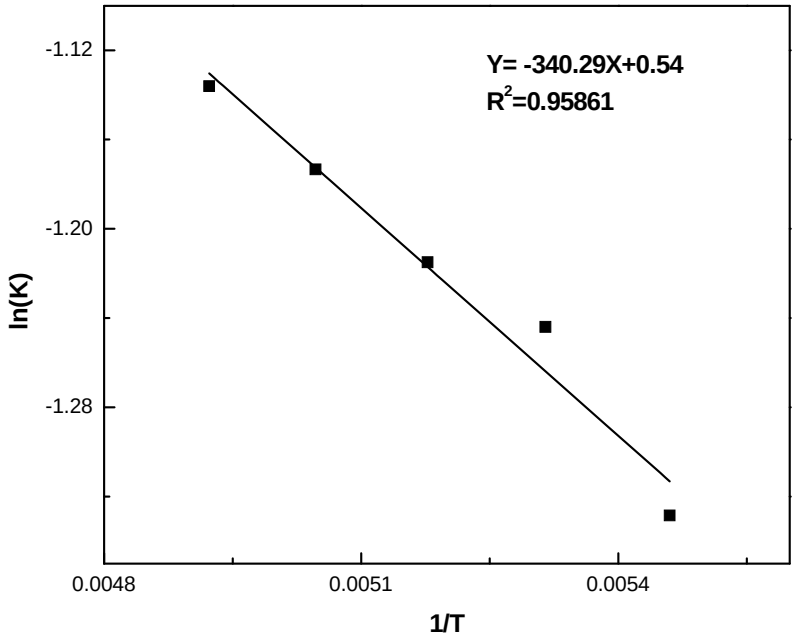

Figure **6-5**: Van't Hoff plot of the Equilibrium for **3** + C_2H_4 ⇌ **4** from −90 °C to −70 °C

Determination of the equilibrium constant between (P~SO_3)Pd($CH_2CH_2C(O)CH_3$) 3 and (P~SO_3)Pd($CH_2CH_2C(O)CH_3$)(CO) 5

Again, the five-membered chelate **3** was generated in situ using the above method. Subsequent exposure of **3** to CO confirmed generation of an equilibrium mixture of **3** and **5**. The NMR data of **5** was listed in the experimental section. The temperature dependent equilibrium was studied in CD_2Cl_2 from −90 °C to −70 °C. The Van't Hoff plot (Figure **6-5**) gives $\Delta H^o = 3.2 \pm 0.2$ kcal/mol and $\Delta S^o = 17.2 \pm 1.2$eu. The calculated equilibrium constant K_1 at 25 ^oC is 27.4 M^{-1}.

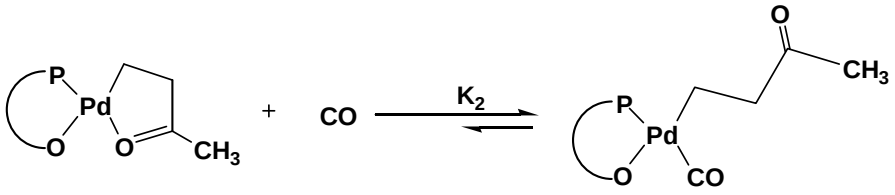

3 **5**

Although impure starting materials **3** was used here, the existence of carbonyl complex **2** would not influence the equilibrium because double CO insertion is kinetically disfavored. Overall the binding equilibrium constant $K_{eq} = K_2/K_1$ was underestimated.

Table **6-3**: Equilibrium constants for **3** + CO ⇌ **5** from −90 °C to −70 °C.

Temperature (°C)	K_2 (M^{-1})	[5] : [3]	[CO] (M)
183	0.919	0.0194	0.0211
188	1.215	0.0257	0.02115
193	1.406	0.0298	0.02119
198	1.916	0.0407	0.02124
203	2.151	0.0458	0.02129

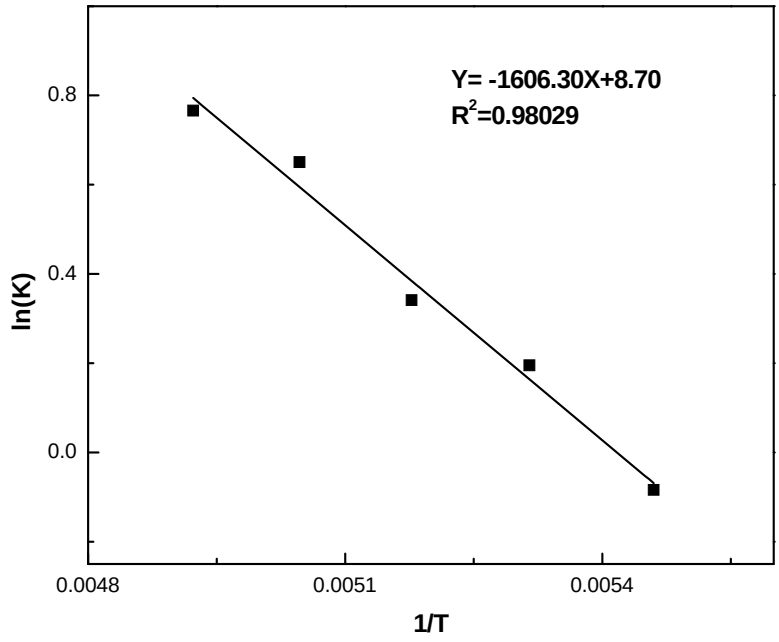

Figure **6-6**: Van't Hoff plot of the equilibrium **3** + CO ⇌ **5** from −90 °C to −70 °C.

Determination of the rate of ethene migratory insertion to 1

The rate of ethene migratory insertion into the methyl complex, **1**, was followed by monitoring the decrease in the Pd–CH_3 ^{1}H NMR resonance. First order kinetics was observed, and the rate was independent of ethene concentration, which is presumably because ethene insertion is slower than coordination to the palladium center. The Eyring plot (Figure **6-7**) gives the activation parameters of $\Delta H^{\ddagger} = 17.7 \pm 1$ kcal/mol and $\Delta S^{\ddagger} = -13.6 \pm 4$ eu.

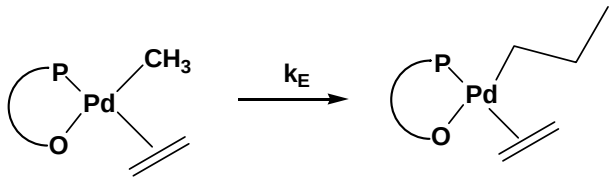

1 **6**

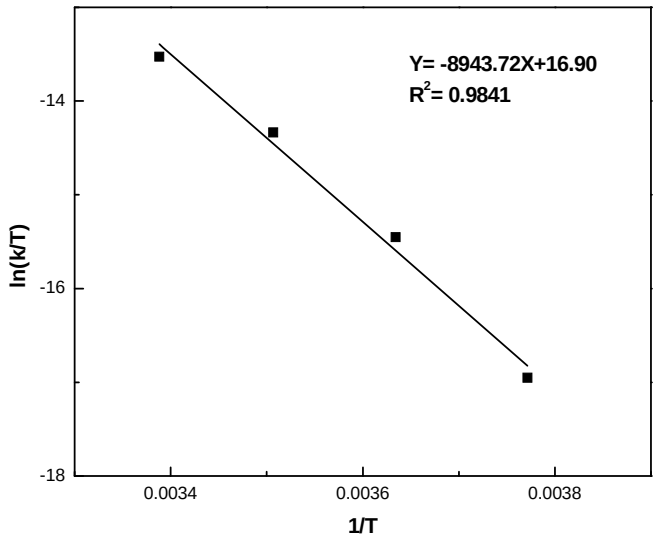

Figure **6-7**: Eyring plot for the migratory insertion reaction **1** + C_2H_4 → **6**.

Determination of the rate of CO migratory insertion to 1

The rate of CO migratory insertion into the methyl complex, **1**, was followed by monitoring the decrease in the ^{1}H resonance of the Pd–CH_3. First order kinetics were observed under pseudo-steady-state conditions for CO, and the rate is first-order in CO. The Eyring plot (Figure **6-8**) yields the activation parameters of $\Delta H^{\ddagger}$ = 15.9 ±1 kcal/mol and $\Delta S^{\ddagger}$ = −3.1±0.5 eu.

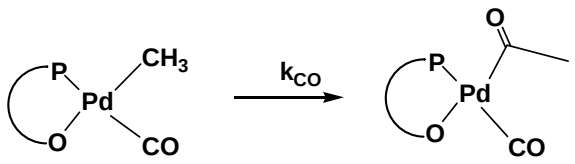

1 **7**

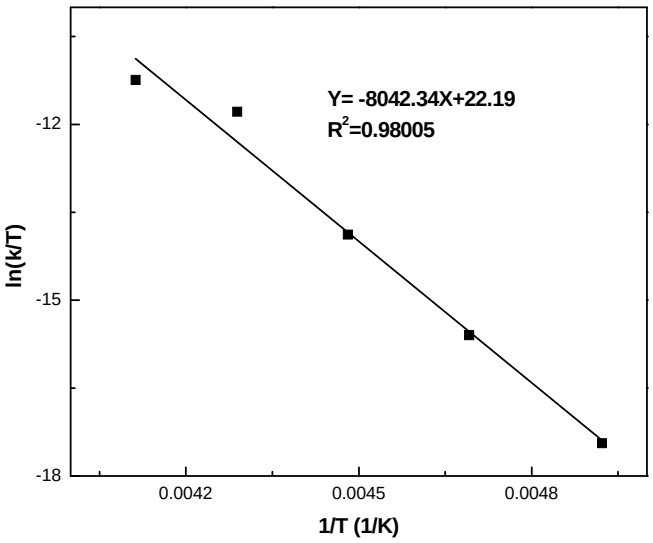

Figure **6-8**: Eyring plot for the migratory insertion reaction **1** + CO → **7**.

The Complete Catalytic Cycle

The ($P\sim SO_3^-$) ligand has the unique ability to produce non-alternating polyketone. We have found that one reason for this non-alternating behavior is that the difference between CO and ethene's affinity for binding to the palladium center is not as dramatic as in other palladium catalyst systems.[5,13] The ratio of the CO and ethene binding constants, K_{eq}, is ~50:1 at 25 °C, compared to a ratio of $\sim 10^4$:1 for palladium complexes bearing a bidentate nitrogen ligand[5] or a bidentate phosphine ligand[13]. As discussed by others, the extent of double ethene insertion was controlled by two factors: the equilibrium ratio of the alkyl carbonyl (**9**) and alkyl olefin (**8**) complexes and the relative rates of migratory insertion of these two species. The factors controlling the ratio of normal propagation to double ethene insertion are illustrated by Eq. 1.

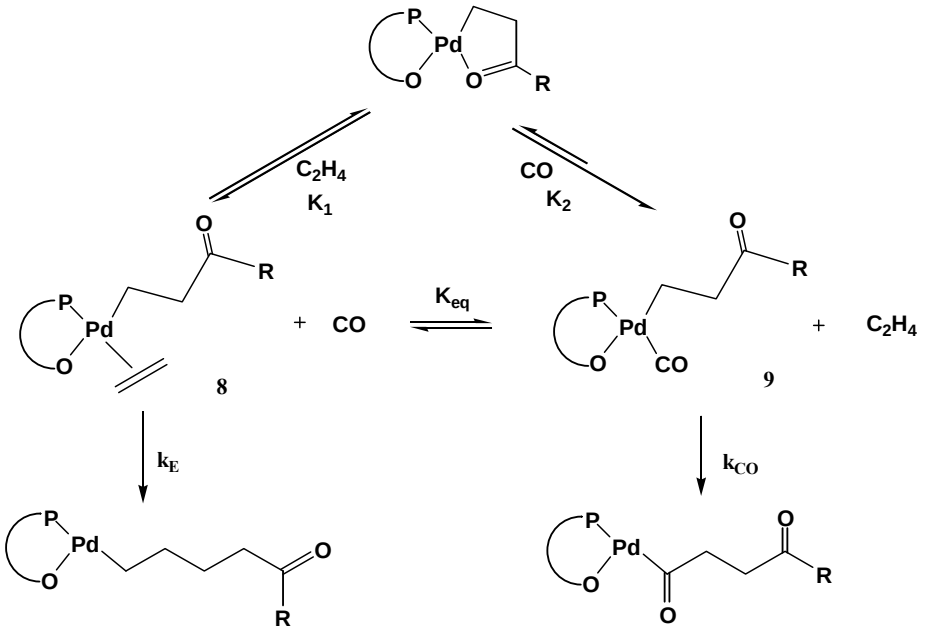

Scheme 6-2: The complete catalytic cycle of the non-alternating copolymerization of CO and ethene.

$$\frac{\text{normal propagation}}{\text{double } C_2H_4 \text{ insertion}} = \left(\frac{[\mathbf{9}]}{[\mathbf{8}]}\right)\left(\frac{k_{CO}}{k_E}\right)$$

$$= K_{eq}\left(\frac{[CO]}{[C_2H_4]}\right)\left(\frac{k_{CO}}{k_E}\right) = \left(\frac{K_2}{K_1}\right)\left(\frac{[CO]}{[C_2H_4]}\right)\left(\frac{k_{CO}}{k_E}\right)$$

$$\approx (50)\left(\frac{7.3\times10^{-3}\ \text{M}}{0.11\ \text{M}}\right)(4000) \approx 10^4$$

Equation 6-1. Determination of the ratio of alternating to non-alternating propagation from the rates of migratory insertion and monomer binding equilibrium constant.

The ratio of [**9**]:[**8**] was estimated from the equilibrium constant K_{eq}, multiplied by the ratio of [CO]:[C_2H_4]. The ratio of the relative propagation rates was estimated from the kinetics study of migratory insertion of CO and ethene as ~4000:1 at 25 °C. Therefore, one double ethene insertion will occur for every 10^4 alternating insertions with a 1:1 monomer feed ratio (1 atm, 25 °C). This is significantly less than either ~10^5 reported for the bidentate phosphine system[13] or ~10^6 reported for the bidentate nitrogen system[5].

6.3 Conclusion

A series of polyketones with very low CO content were synthesized using a palladium catalyst bearing a (P~SO_3^-) ligand by varying the monomer feed ratio and reaction conditions. We demonstrate that the reasons for the non-alternation in this system are more complicated than just the destabilization of the five-membered chelate resting state in the catalytic cycle. The unusually small difference in CO and ethene binding affinity toward the catalyst also plays an important role in determining the polymer composition. The kinetic and thermodynamic data allow us to estimate the fraction of non-alternation due to double ethene insertion during the copolymerization.

6.4 Experimental Procedure

6.4.1 Materials

The following information applies to all experimental procedures unless otherwise noted. Chemical manipulations were performed under a dry nitrogen atmosphere using a glove box or Schlenk techniques. All solvents, with the exception of NMR solvents, were distilled over CaH_2 and degassed using the freeze-pump-thaw technique. Ultra high purity ethene and ultra high purity carbon monoxide were obtained from MG Industries and used without further purification. Isotopically enriched solvents were obtained from Cambridge Isotope Laboratories and used without further purification. Palladium acetate (99%) was purchased from Johnson Matthey and used as received. The phosphine-sulfonate ligand (P~SO_3H) was synthesized following the literature procedure.[10] The pyridine complex (P~SO_3)Pd(Me)(Py), **1**, was synthesized following the literature procedure.[11]

6.4.2 Instrumentation

NMR analysis was performed using a Bruker DPX-300 spectrometer equipped with a variable-temperature, multi-nuclear probe at 300.13 MHz for ^{1}H-, 121.49 MHz for ^{31}P- or 75.4 MHz for ^{13}C NMR spectra. ^{31}P- and ^{13}C NMR experiments were conducted with proton decoupling.

Differential scanning calorimetry was performed by heating 3 mg copolymer sample at a rate of 20 °C/min from 40 °C to 300 °C using a TA Instruments model DSC Q100.

IR analysis was performed using a Varian FTS 7000 series DigiLab FT-IR spectrometer equipped with a ceramic IR source, KBr beamsplitter, deuterated tri-glycine sulfate detector and 632.8 nm HeNe laser with a 5 KHz laser modulation frequency. The sample chamber was flushed with dry nitrogen and data was collected from 4000–900 cm^{-1} with a resolution of 1 cm^{-1}.

6.4.3 General procedure for copolymerization of ethene and carbon monoxide

All bulk polymerization reactions were carried out in an open 50 mL serum bottle placed in a 125 mL autoclave with magnetic stirring. The bottle was charged with 22 mg (0.10 mmol) $Pd(OAc)_2$ and 40 mg (0.10 mmol) P~SO_3H ligand and 10 mL dichloromethane. The bottle was placed in the autoclave, and removed from the glove box. The autoclave was then charged with desired amount of ethene and carbon monoxide. The autoclave was placed in a 90 °C oil bath with magnetic stirring for 1.5 h. At the end of the period, the autoclave was cooled to room temperature, vented to the atmosphere, and opened. The resulting polymer was precipitated with acidified methanol, collected by vacuum filtration, and dried under high vacuum overnight before analysis.

Polymers were dissolved in tetrachloroethane-d_2 at 100 °C for NMR analysis. Carbon monoxide incorporation was determined by the integration of the CH_2 protons adjacent the carbonyl group (2.7–2.3 ppm) and those not adjacent to the carbonyl group (1.5–1.2 ppm).

6.4.4 Themodynamics of (P~SO_3)Pd($CH_2CH_2{}^{13}C(O)CH_3$), 3, + C_2H_4 ⇌ P~SO_3)Pd($CH_2CH_2{}^{13}C(O)CH_3$)(C_2H_4), 4

In order to improve ^{13}C NMR sensitivity, complex **3** was formed from **2**, which had been synthesized using the previous procedure with isotopically enriched ^{13}CO. A solution of **3** and

unreacted **2** in 0.7 mL CD_2Cl_2 (total concentration 0.046 M) was added to a high pressure NMR tube (Wilmad, Quick Pressure Valve, 5 mm outer diameter, 8 inch length, 0.77 mm wall thickness) in the glove box. The tube was charged to 80 psi with ethene at −78 °C. The equilibrium constant for the reaction **3** + C_2H_4 ⇌ **4** was determined from −90 °C to −70 °C (See Supporting Information). The concentrations of **3** and **4** were determined by ^{13}C NMR integration of the carbonyl resonances at 210 ppm and 201 ppm, respectively. The ethene concentration was calculated from ^{1}H NMR integration of the peak at 5.5 ppm.

Thermodynamic parameters were determined from the Van't Hoff plot (Figure 6-5): ΔH^{o}= 0.68 ± 0.07 kcal/mol and ΔS^{o}= 1.1 ± 0.3 eu.

6.4.5 Themodynamics of (P~SO_3)Pd($CH_2CH_2{}^{13}C(O)CH_3$), 3 + CO ⇌ (P~SO_3)Pd($CH_2CH_2{}^{13}C(O)CH_3$)(CO), 5

In order to improve ^{13}C NMR sensitivity, complex **3** was formed from **2**, which had been synthesized using the previous procedure with isotopically enriched ^{13}CO. A solution of **3** and unreacted **2** in 0.7 mL CD_2Cl_2 (total concentration 0.046 M) was added to a high pressure NMR tube in the glove box. The tube was charged to 50 psi with CO at −78 °C. The equilibrium constant for the reaction **3** + CO ⇌ **5** was determined from −90 °C to −70 °C (See Supporting Information). The concentrations of **3** and **5** were determined by ^{13}C NMR integration of the carbonyl resonances at 210 ppm and 201 ppm, respectively.

CO concentration was determined using the equation reported by Bryndza[16]:

$$[CO]_{sat} = (2.75 \times 10^{-6})T + (6.45 \times 10^{-3})$$

Where T is the temperature in °C.

Thermodynamic parameters were determined from the Van't Hoff plot (Figure 6-6): $\Delta H^{o} = 3.2 \pm 0.2$ kcal/mol and $\Delta S^{o} = 17.2 \pm 1.2$eu.

6.4.6 Kinetics study of migratory insertion of ethene into (P~SO_3)Pd(CH_3)(Py), 1

A solution of **1** (28 mg, 0.065 M) in 0.7 mL CD_2Cl_2 solution was added to a high pressure NMR tube in the glove box. The tube was charged to 40 psi with ethene at −78 °C. The sample was placed in a pre-cooled NMR probe, and the decrease in Pd–CH_3 intensity of **1** was followed by ^{1}H NMR spectroscopy. The plot of ln[Pd–CH_3] of **1** vs. time was observed for different ethene concentrations. Kinetics runs with 40 psi and 80 psi ethene at -10 ^{o}C give $k_{obs} = 1.19 \times 10^{-5}$ s^{-1} and 1.23×10^{-5} s^{-1}, which revealed that the rate of the reaction was independent of [C_2H_4].

A series of kinetics experiments conducted over a temperature range of 40 °C afforded a linear fit for the Eyring plot (Figure **6-7**). These data give $\Delta H^{\ddagger} = 17.7 \pm 1$ kcal/mol and $\Delta S^{\ddagger} = -13.6 \pm 4$ eu**.**

6.4.7 Kinetics study of migratory insertion reaction of CO into (P~SO_3)Pd(Py)(CH_3), 1

A solution of **1** in 0.7 mL CD_2Cl_2 (28 mg, 0.065 M) was added to a high pressure NMR tube in the glove box. The tube was charged to 40 psi with CO at −78 °C. The sample was placed in a pre-cooled NMR probe, and the decrease in Pd–CH_3 intensity of **1** was followed by ^{1}H NMR spectroscopy. The plot of ln[Pd–CH_3] of **1** vs. time was observed for different CO concentrations. Kinetics runs with 40 psi and 80 psi CO at -40 ^{o}C give $k_{obs} = 3.05 \times 10^{-5}$ s^{-1} and 6.04×10^{-5} s^{-1}, which revealed that the rate of the reaction was first order of CO.

A series of kinetics experiments conducted over a temperature range of 50 °C afforded a linear fit from the Eyring plot (Figure **6-8**). These data give $\Delta H^{\ddagger} = 15.9 \pm 1$ kcal/mol and $\Delta S^{\ddagger} = -3.1 \pm 0.5$ eu.

6.4.8 NMR data

All spectra were recorded at room temperature except where stated otherwise.

(P~SO_3)Pd(CH_3)(Py), 1. ^{1}H NMR data (CD_2Cl_2): δ 7.0–8.2 ppm (m, 12H, aromatic), δ 8.7 ppm, 7.6 ppm, 7.2 ppm (m, 5H, pyridine), δ 3.7 ppm (s, 6H, –OCH_3), δ 0.2 ppm (s, 3H, Pd–CH_3). ^{31}P NMR data (CD_2Cl_2): δ 22.7 ppm (s).

(P~SO_3)Pd(C(O)CH_3)(Py), 2. Generated by CO insertion into **1**. ^{1}H NMR data (CD_2Cl_2): δ 7.0–8.2 ppm (m, 12H, aromatic), δ 8.7 ppm, 7.6 ppm and 7.2 ppm (m, 5H, pyridine), δ 3.7 ppm (s, 6H, –O*CH_3*), δ 1.8 ppm (s, 3H, Pd–C(O)*CH_3*). ^{13}C NMR data (CD_2Cl_2, recorded at −70 °C): δ229 ppm (br, Pd–*C*(O)CH_3). ^{31}P NMR data (CD_2Cl_2): δ 10.9 ppm (s).

(P~SO_3)Pd(CH_2CH_2C(O)CH_3), 3. Generated by ethene insertion into **2**. ^{1}H NMR data (CD_2Cl_2): δ 7.0–8.2 ppm (m, 12H, aromatic), δ 3.7 ppm (s, 6H, –O*CH_3*), δ 2.1 ppm (br m, Pd–CH_2*CH_2*C(O)CH_3), δ 1.9 ppm (s, 3H, Pd–CH_2CH_2C(O)*CH_3*), δ 1.3 ppm (br m, Pd–*CH_2*CH_2C(O)CH_3). ^{13}C NMR data (CD_2Cl_2, recorded at −70 °C): δ210 ppm (br, Pd–CH_2CH_2*C*(O)CH_3). ^{31}P NMR data (CD_2Cl_2): δ 23.3 ppm (s).

(P~SO_3)Pd(CH_2CH_2C(O)CH_3)(C_2H_4), 4. Generated by ethene coordination to **3**. ^{1}H NMR data (CD_2Cl_2, recorded at −70 °C): δ 7.0–8.2 ppm (m, 12H, aromatic), δ 5.5 ppm (s, 4H, C_2*H_4*), δ 3.7 ppm (br m, 6H, –O*CH_3*), δ 1.5-1.7 ppm (br m, Pd–CH_2*CH_2*C(O)CH_3), δ 1.4 ppm (s, 3H, Pd–CH_2CH_2C(O)*CH_3*), δ 0.8–1.1 ppm (br m, Pd–*CH_2*CH_2C(O)CH_3). ^{13}C NMR data (CD_2Cl_2,

recorded at −70 °C): δ201 ppm (br, Pd–CH_2CH_2*C*(O)CH_3). ^{31}P NMR data (CD_2Cl_2, recorded at −70 °C): δ 27.0 ppm (br).

(P~SO_3)Pd($CH_2CH_2C(O)CH_3$)(CO), 5. Generated by CO coordination to **3**. ^{1}H NMR data (CD_2Cl_2, recorded at −70 °C): δ 7.0–8.2 ppm (m, 12H, aromatic), δ 3.7 ppm (br m, 6H, –OC*H*$_3$), δ 1.5-1.7 ppm (br m, Pd–CH_2C*H*$_2$C(O)CH_3), δ 1.4 ppm (s, 3H, Pd–$CH_2CH_2C(O)$*CH*$_3$), δ 0.8–1.1 ppm (br m, Pd–C*H*$_2CH_2C(O)CH_3$). ^{13}C NMR data (CD_2Cl_2, recorded at −70 °C): δ201 ppm (br, Pd–CH_2CH_2*C(O)*CH_3). ^{31}P NMR data (CD_2Cl_2, recorded at −70 °C): δ 26.6 ppm (br).

(P~SO_3)Pd($CH_2CH_2CH_3$)(C_2H_4), 6. Generated from the migratory insertion of ethene into **1**. ^{1}H NMR data (CD_2Cl_2): δ 7.0–8.2 ppm (m, 12H, aromatic), δ 3.7 ppm (br m, 6H, –OC*H*$_3$), δ 1.3 ppm (br m, Pd–CH_2C*H*$_2CH_3$), δ 1.0 ppm (s, 3H, Pd–CH_2CH_2C*H*$_3$), δ 0.8 ppm (br m, Pd–C*H*$_2CH_2CH_3$). ^{31}P NMR data (CD_2Cl_2): δ 27.1 ppm (br).

(P~SO_3)Pd(C(O)CH_3)(CO), 7. Generated from the migratory insertion of CO into **1**. ^{1}H NMR data (CD_2Cl_2): δ 7.0–8.2 ppm (m, 12H, aromatic), δ 3.7 ppm (br m, 6H, –OC*H*$_3$), δ 1.8 ppm (s, 3H, Pd–C(O)C*H*$_3$). ^{31}P NMR data (CD_2Cl_2): δ 11.4 ppm (br).

6.5 References

1. Catalytic Synthesis of Alkene-Carbon Monoxide Copolymers and Cooligomers; Sen, A., Ed.; Catalysis by Metal Complexes 27; Kluwer Academic: Dordrecht, 2003.
2. Mul, W. P.; Oosterbeck, H.; Betel, G. A.; Kramer, G.-J.; Drent, E. *Angew. Chem., Int. Ed.* **2000**, *39*, 1848–1851.
3. Drent, E. *Pure Appl. Chem.* **1990**, *62*, 661.
4. Rix, F. C.; Brookhart, M. *J. Am. Chem. Soc*. **1995**, *117*, 1137.
5. Rix, F. C.; Brookhart, M.; White, P. S. *J. Am. Chem. Soc*. **1996**, *118*, 4746–4764.
6. Nozaki, K.; Sato, N.; Tonomura, Y.; Yasutomi, M.; Takaya, H.; Hiyama, T.; Matsubara, T.; Koga, N. *J. Am. Chem. Soc*. **1997**, *119*, 12779.
7. Margl, P.; Ziegler, T. *J. Am. Chem. Soc*. **1996**, *118*, 7337.
8. Chen, J. T.; Sen, A. *J. Am. Chem. Soc*. **1984**, *106*, 1506.
9. Chen, J. T.; Vetterand, W. M.; Whittle R. R.; Sen, A. *J. Am. Chem. Soc*. **1987**, *109*, 148.
10. Drent, E.; van Dijk, R.; van Ginkel, R.; van Oort, B.; Pugh, R. I. *Chem. Commun*. **2002**, 964–965.
11. Newsham, D. K.; Borkar, S.; Sen, A.; Cornor, D. M.; Goodall, B. L. *Organometallics*. **2007**, *26*, 3636–3638.
12. Hearley, A. K.; Nowack, R. J.; Rieger, B. *Organometallics*. **2005**, *24*, 2755–2763.
13. Shultz, C. S.; Ledford, J.; DeSimone, J. M.; Brookhart, M. *J. Am. Chem. Soc*. **2000**, *122*, 6351–6356.
14. Haras, A.; Michalak, A.; Rieger, B.; Ziegler, T. *J. Am. Chem. Soc*. **2005**, *127*, 8765–8774.
15. Lai, T. W.; Sen, A. *Organometallics*. **1984**, *3*, 866–870.
16. Bryndza, H. E. *Organometallics*. **1985**, *4*, 1686–1687.

VITA

Rong Luo

Rong Luo received her Master Degree in Organic Chemistry from Huazhong University of Science and Technology before she joined Penn State University in August 2004. She started her graduate research under the supervision of Dr. Ayusman Sen. Her research is mainly focused on the copolymerization of polar and non-polar monomers. While at Penn State, she published five research papers, and she is also the recipient of the Dalalian research award in 2007. Rong Luo received her Ph.D in the fall of 2008. After graduation, Rong joined Celanese Corporation as a research chemist.